

## FEATURE ARTICLE



Cite this: *Chem. Commun.*, 2014, 50, 12234

## Fluorescent probes for hydrogen sulfide detection and bioimaging

Fabiao Yu,<sup>a</sup> Xiaoyue Han<sup>ab</sup> and Lingxin Chen<sup>\*a</sup>

In comparison with other biological detection technologies, fluorescence bioimaging technology has become a powerful supporting tool for intracellular detection, and can provide attractive facilities for investigating physiological and pathological processes of interest with high spatial and temporal resolution, less invasiveness, and a rapid response. Due to the versatile roles of hydrogen sulfide (H<sub>2</sub>S) in cellular signal transduction and intracellular redox status regulation, fluorescent probes for the detection of this third signalling gasotransmitter have rapidly increased in number in recent years. These probes can offer powerful means to investigate the physiological actions of H<sub>2</sub>S in its native environments without disturbing its endogenous distribution. In this feature article, we address the synthesis and design strategies for the development of fluorescent probes for H<sub>2</sub>S based on the reaction type between H<sub>2</sub>S and the probes. Moreover, we also highlight fluorescent probes for other reactive sulfur species, such as sulfane sulfurs and SO<sub>2</sub> derivatives.

Received 4th May 2014,  
Accepted 6th June 2014

DOI: 10.1039/c4cc03312d

www.rsc.org/chemcomm

### Introduction

Fluorescence bioimaging technology can be distinguished readily amongst biological detection technologies by its many advantages, such as good sensitivity, excellent selectivity, rapid response, and non-invasive detection. In biological systems, features of physiologically active species include low concentration, high reactivity and short lifetimes. Therefore, it still

remains a huge challenge to determine the intracellular concentration of these species accurately. In order to meet these urgent needs, reaction-based fluorescent probes have emerged.<sup>1,2</sup>

In general, the design and synthetic strategies of these probes depend on the chemical properties of the physiologically active species. The reaction-based fluorescent probes are mainly composed of two moieties: the fluorescence signal transducer and the fluorescence modulator (Fig. 1). The fluorescence signal transducer moiety transduces molecular recognition into a fluorescence signal that can be detected. It is essential to choose a suitable fluorophore platform as the signal transducer. High quantum yield, photostability and bio-compatibility are critical for bioimaging, such that the minimum dosage of the probe can avoid disturbing the natural

<sup>a</sup> Key Laboratory of Coastal Environmental Processes and Ecological Remediation, The Research Center for Coastal Environmental Engineering and Technology of Shandong Province, Yantai Institute of Coastal Zone Research, Chinese Academy of Sciences, Yantai 264003, China. E-mail: lxchen@yic.ac.cn

<sup>b</sup> University of Chinese Academy of Sciences, Beijing 100049, China



Fabiao Yu

Fabiao Yu received his MS from Shandong Normal University in 2009. He then received his PhD degree from the Dalian University of Technology and Dalian Institute of Chemical Physics, Chinese Academy of Sciences, in 2013. He is currently an associate professor at the Yantai Institute of Coastal Zone Research, Chinese Academy of Sciences. His research interests focus on functional probe molecules, mainly in fluorescence and phosphorescence analysis.



Xiaoyue Han

Xiaoyue Han received her BS from Qufu Normal University, in 2013. She is currently a PhD candidate under the supervision of Prof. Lingxin Chen at the Yantai Institute of Coastal Zone Research, Chinese Academy of Sciences. Her research interests focus on the design and synthesis of fluorescent probes.

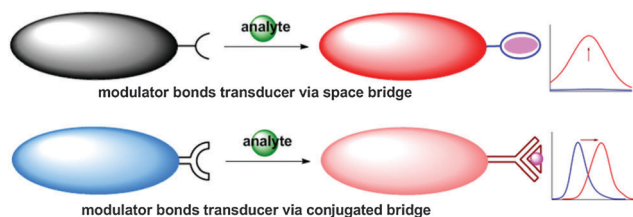
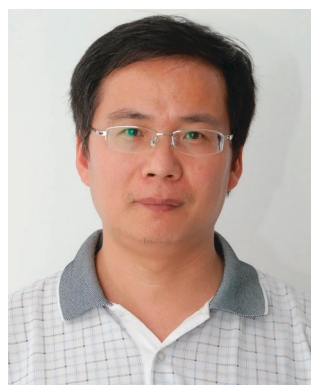


Fig. 1 Schematic illustration of the design of fluorescent probes.

distribution of the physiologically active species. The fluorescence modulator moiety manipulates the molecular recognition process. A desirable fluorescence modulator can only be triggered by a single reaction switch. The selected reaction is also screened to ensure it possesses reasonable reaction kinetics under physiological conditions. After integrating the modulator into the transducer *via* a conjugated or a space bridge, a reaction-based fluorescent probe is generated (Fig. 1). All the features of the fluorescence response can be employed as outputs based on their signal changes, such as absorption, emission spectra, and fluorescence lifetime. It is generally recognized that turn-on fluorescent probes are more efficient compared with turn-off probes. Turn-on signals provide ease of measuring low concentrations against a dark background, which can reduce false positive signals and increase sensitivity. Appropriate fluorescent probes also possess near-infrared absorption and emission spectra (including two-photon and multi-photon), because the light in this region shows maximized tissue penetration while minimizing the absorbance of heme in hemoglobin and myoglobin, water, and lipids. Moreover, ratiometric probes benefit from measuring the ratio of the emission intensity at two different wavelengths, since the interference caused by factors such as uneven loading and



Lingxin Chen

Lingxin Chen received his PhD from the Dalian Institute of Chemical Physics, Chinese Academy of Sciences, in 2003. After two years of postdoctoral experience at the Department of Chemistry, Tsinghua University, China, he worked first as a BK21 researcher and then as a research professor at the Department of Applied Chemistry, Hanyang University, Ansan, Korea, in 2006. Now he is a professor at the Yantai Institute of Coastal Zone Research, Chinese

Academy of Sciences. His research interests include the study of novel properties of materials such as functionalized nanoparticles for developing nanoscale biochemical analysis methods, molecular imprinting based sample pre-treatment technologies combined with chromatography, and the mechanism of microbial degradation of pollutants.

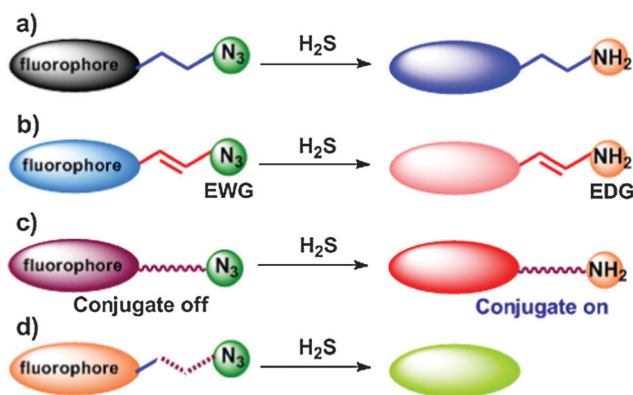


Fig. 2 Summary of strategies for fluorescent probes based on reducing azides to amines.

the inhomogeneous distribution of fluorescent probes in cells can be cancelled out. Finally, the probes should have low cytotoxicity and appropriate water solubility.

Intracellular reactive sulfur species (RSS) is a general term for sulfur-containing biomolecules. These molecules play critical roles in physiological and pathological processes. Glutathione (GSH), the most abundant intracellular nonprotein thiol, can control intracellular redox activity, intracellular signal transduction, and gene regulation. Cysteine (Cys) is implicated in slow growth in children, liver damage, skin lesions, and loss of muscle and fat. Homocysteine (Hcy) is a risk factor for Alzheimer's disease and cobalamin (vitamin B12) deficiency.<sup>3</sup> H<sub>2</sub>S has been identified as the third gasotransmitter following nitric oxide (NO) and carbon monoxide (CO). At physiological levels, H<sub>2</sub>S regulates the intracellular redox status and fundamental signalling processes, including regulation of vascular tone, myocardial contractility, neurotransmission, and insulin secretion. Abnormal levels of H<sub>2</sub>S in cells can induce many diseases, such as Alzheimer's disease, liver cirrhosis, gastric mucosal injury and arterial and pulmonary hypertension.<sup>4</sup> In recent years, the development of fluorescent probes for H<sub>2</sub>S has rapidly increased, benefiting from the chemical reactions of H<sub>2</sub>S.

The fluorescent probes for GSH, Cys and Hcy have been well reviewed.<sup>5,6</sup> Hitherto, there have been few reviews on the progress of fluorescent probes for H<sub>2</sub>S.<sup>7</sup> Now, we overview the synthesis and design strategies for the development of fluorescent probes based on the reaction type between H<sub>2</sub>S and the probes. We classify these probes according to their reaction type with H<sub>2</sub>S: (a) H<sub>2</sub>S reductive reactions: reducing azides to give amines, reducing nitro/azanol to give amines, and reducing selenoxide to give selenide; (b) H<sub>2</sub>S nucleophilic reactions: Michael addition reactions, dual nucleophilic reactions, double bond addition reactions, and thiolysis reactions; (c) copper sulfide precipitation reaction. Moreover, we also introduce fluorescent probes for other reactive sulfur species, such as sulfane sulfurs and SO<sub>2</sub> derivatives. The detection of sulfane sulfurs is mainly based on the nucleophilic addition reaction, and the detection of SO<sub>2</sub> derivatives is based on their nucleophilic and reductive properties.

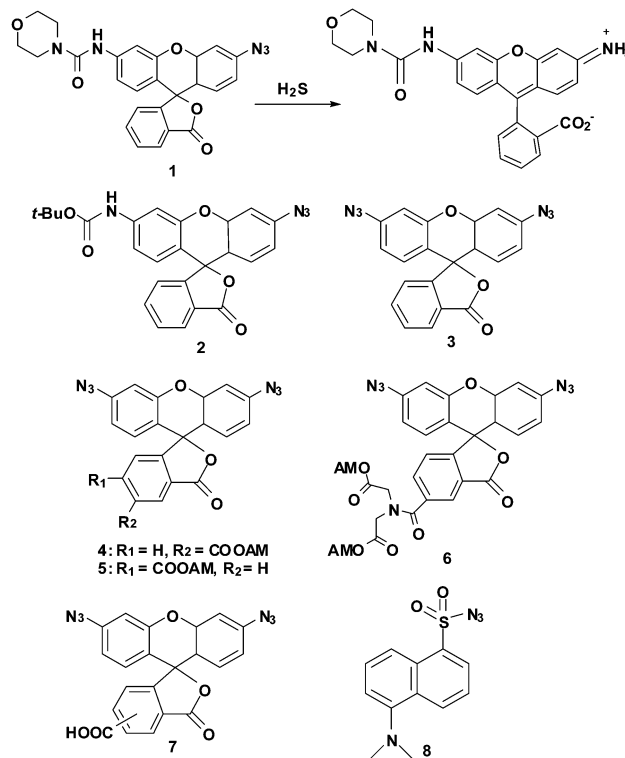
## Fluorescent probes based on reducing azides to amines

Azides and other oxidized nitrogen species can be reduced to amines by  $\text{H}_2\text{S}$  faster than by GSH and other thiols, signifying a promising method for  $\text{H}_2\text{S}$  detection. Upon reduction by  $\text{H}_2\text{S}$ , the electron-withdrawing azido group will be converted into an electron-donating amino group. Therefore, exploiting the electron-donating ability of different substituent groups will result in versatile fluorescent probes (Fig. 2). The fluorescent probes employing the photoinduced electron transfer (PET) mechanism are typically constructed by connecting an electron donor/acceptor recognition group to a fluorophore *via* a space bridge. The design principles of such probes are clear, and the resulting processes will quench or increase the fluorescence of these probes (Fig. 2a). The fluorescent probes that adopt an internal charge transfer (ICT) mechanism typically contain a strong push-pull electronic system, wherein the electron donating group (EDG) and the electron withdrawing group (EWG) are conjugated to the fluorophore. Depending on the ICT mechanism, ratiometric probes can be readily available (Fig. 2b). The changes in the  $\pi$ -conjugated systems triggered by chemical reactions are often followed by a notable alteration in spectroscopic properties, which is advantageous to obtain turn-on/ratiometric fluorescent probes (Fig. 2c). Moreover, design strategies that take advantage of protecting group chemistry will result in excellent probes (Fig. 2d). The approaches mentioned above have since been widely adopted for  $\text{H}_2\text{S}$  detection (Fig. 2).

Chang *et al.* have exploited the selective  $\text{H}_2\text{S}$ -mediated reduction of azides to develop a series of fluorescent probes for intracellular  $\text{H}_2\text{S}$  detection (1–6).<sup>8,9</sup> The fluorophores of these probes were based on Rhodamine 110. The detection mechanism was illustrated in Fig. 2c. After caging Rhodamine 110 by azides at the 3 or 6 positions, the probes 1–6 adopted a closed lactone conformation, and exhibited no absorption features. When azides were reduced to amines by  $\text{H}_2\text{S}$ , the spiro-rings of 1–6 opened, and the  $\pi$ -conjugated structure was recovered. Therefore, these  $\text{H}_2\text{S}$  probes gave a turn-on response. Probes 1 and 2 could detect  $\text{H}_2\text{S}$  in live HEK293T cells using confocal microscopy, and it took about 1 h to saturate the fluorescence response. Under test conditions, Probe 1 gave a fluorescence quantum yield,  $\Phi$ , of 0.60. For Probe 2,  $\Phi = 0.51$ . The detection limit of 1 was  $10 \mu\text{M}$ . However, the concentration of  $\text{H}_2\text{S}$  changed acutely in cells, and it was difficult for 1 and 2 to capture  $\text{H}_2\text{S}$  opportunely in cells. Later, the same group optimized these design strategies and improved the sensitivity and cellular retention in their new probes. They reported bis-azido probes (3–6) for increasing  $\text{H}_2\text{S}$  sensitivity, and they incorporated an acetoxymethyl ester-protected carboxy group into the new probes to increase cellular trappability (4–6). It is worth noting that probe 6 could, directly and in real-time, detect endogenous  $\text{H}_2\text{S}$  which was produced in live human umbilical vein endothelial cells upon stimulation with vascular endothelial growth factor (VEGF). The detection limit of 6 was 500 nM. They also revealed that endogenous  $\text{H}_2\text{S}$  production was related to NADPH oxidase-derived hydrogen peroxide

( $\text{H}_2\text{O}_2$ ). This experimental result would establish a link for  $\text{H}_2\text{S}/\text{H}_2\text{O}_2$  crosstalk. Under test conditions, probes 3, 4, 5 and 6 displayed fluorescence quantum yields of 0.92, 0.18, 0.18 and 0.17, respectively. Based on Rhodamine 110 as the fluorophore, Sun *et al.* also developed a fluorescent probe 7 to trap intracellular  $\text{H}_2\text{S}$  in HeLa cells.<sup>10</sup> Probe 7 displayed a 120-fold fluorescence enhancement as a turn-on response, and the detection limit was  $1.12 \times 10^{-7} \text{ M}$ .

Wang *et al.* developed a turn-on fluorescent probe 8 for  $\text{H}_2\text{S}$  detection in aqueous solutions, blood serum and whole blood.<sup>11</sup> The detection mechanism of the probe was illustrated in Fig. 2a. When the azido group was attached to a strongly electron-withdrawing dansyl fluorophore, the reductive reaction was accelerated. Probe 8 showed a fast response to  $\text{H}_2\text{S}$ , within seconds, which made quantitative  $\text{H}_2\text{S}$  detection possible regardless of the fact that it is rapidly metabolized in biological systems. The detection limit was  $1 \mu\text{M}$  in buffer/Tween and  $5 \mu\text{M}$  in bovine serum. The  $\text{H}_2\text{S}$  concentrations in C57BL6/J mouse model blood were determined to be  $31.9 \pm 9.4 \mu\text{M}$  using 8. The addition of  $\text{H}_2\text{S}$  led to a 40-fold increase in the fluorescence of probe 8.

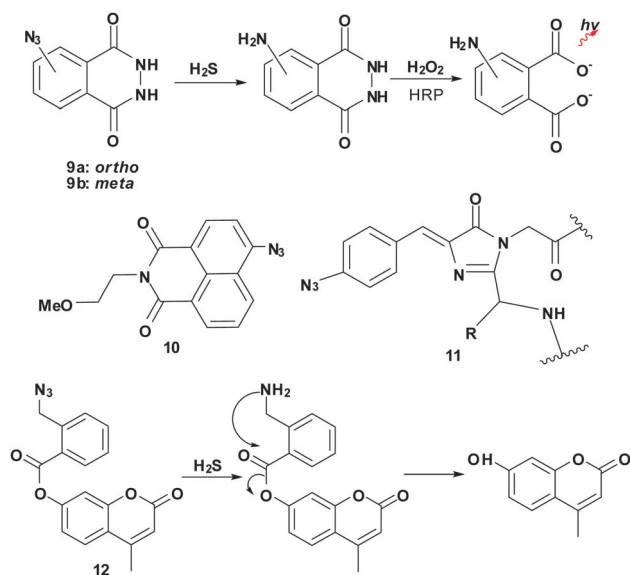


Pluth *et al.* reported two reaction-based chemiluminescent probes for  $\text{H}_2\text{S}$  (9a and 9b).<sup>12</sup> Since chemiluminescence does not require excitation by any source, there is little chance of photodegradation of the probe. Furthermore, chemiluminescent probes can avoid biological background interference. Therefore, chemiluminescent methods can provide high signal-to-noise ratios in  $\text{H}_2\text{S}$  detection. 9a and 9b combined an  $\text{H}_2\text{S}$ -mediated azido group with a luminol derived platform. After reduction by  $\text{H}_2\text{S}$ , chemiluminescence resulted from the oxidation of the

phthalhydrazide moiety, which was oxidized by  $\text{H}_2\text{O}_2$  using horseradish peroxidase (HRP) as a catalyst. Probe **9b** was used to detect enzymatically-produced  $\text{H}_2\text{S}$  from both isolated CSE enzymes and C6 cell lysates. Probes **9a** and **9b** had strong luminescence responses towards  $\text{H}_2\text{S}$ , with 128- and 48-fold increases, respectively. The detection limits of **9a** and **9b** were  $0.7 \pm 0.3$  and  $4.6 \pm 2.0$   $\mu\text{M}$ , respectively. The group also synthesized fluorescent probe **10** based on azido-naphthalimide.<sup>13</sup> When probe **10** reacted with  $\text{H}_2\text{S}$ , the azide was reduced to an amine following a turn-on fluorescent response. Probe **10** could detect  $\text{H}_2\text{S}$  in HeLa cells; however, this was subject to interference from GSH. Probe **10** gave a quantum yield of  $0.096 \pm 0.001$ , and the detection limit was 5–10  $\mu\text{M}$ .

Ai *et al.* reported encoded fluorescent proteins (FPs)-based probe **11** to detect  $\text{H}_2\text{S}$ .<sup>14</sup> FPs can be self-sufficient in generating intrinsic chromophores from polypeptide sequences. They incorporated *p*-azidophenylalanine (*p*AzF) into peptides of FPs to obtain azide-derived chromophores. This genetically encoded probe could be used to monitor  $\text{H}_2\text{S}$  concentration changes in HeLa cells.

Han *et al.* designed and synthesized fluorescent probe **12** based on utilization of *o*-(azidomethyl)benzoyl as the hydroxyl protecting group.<sup>15</sup> The detection mechanism of the probe was illustrated in Fig. 2d. When  $\text{H}_2\text{S}$  triggered the reduction of the azido moiety, the fluorophore 7-hydroxy-4-methylcoumarin was deprotected, and fluorescence was emitted. Probe **12** could be used for imaging  $\text{H}_2\text{S}$  in HeLa cells, and the detection limit was 10  $\mu\text{M}$ .



Han *et al.* reported a colorimetric and ratiometric fluorescent probe **13** for detecting  $\text{H}_2\text{S}$ .<sup>16</sup> The detection mechanism of the probe was illustrated in Fig. 2b. It was anticipated that the modulation of various electron-donating groups on a cyanine dye could affect its intermolecular electron density distribution. Therefore, controlling the electron-donating ability of different substituent groups would result in ICT-induced blue or red shifts in the emission spectrum of cyanine. When  $\text{H}_2\text{S}$  reduced

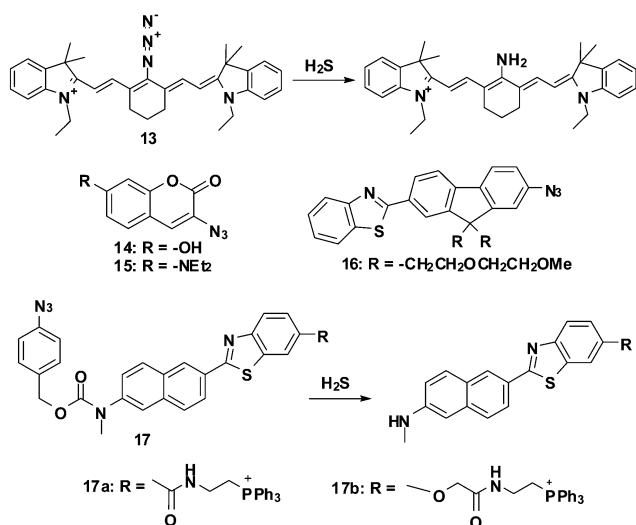
the azide to an amine, the near-infrared heptamethine cyanine platform showed a shift in its emission spectra from 710 nm to 750 nm. The quantum yields of probe **13** and its product changed from 0.11 to 0.12. The probe could evaluate  $\text{H}_2\text{S}$  by fluorescence ratio signals in aqueous solution and fetal bovine serum. Probe **13** could monitor  $\text{H}_2\text{S}$  release by ADT-OH. This probe was able to sense different  $\text{H}_2\text{S}$  levels in RAW 264.7 cells using confocal microscopy ratiometric imaging. The detection limit was 0.08  $\mu\text{M}$ .

Li *et al.* reported two coumarin-based fluorescent probes **14** and **15** for the detection of  $\text{H}_2\text{S}$ .<sup>17</sup> Probes **14** and **15** were both caged by an azido group. When reduced by  $\text{H}_2\text{S}$ , probe **15** showed a larger increase in fluorescence intensity, because the electron-donating ability of  $-\text{NET}_2$  was stronger than that of  $-\text{OH}$ , and was controlled by stronger ICT effects. **14** and **15** gave quantum yields of  $0.16 \pm 0.013$  and  $0.58 \pm 0.02$ , respectively, and probe **15** could detect  $\text{H}_2\text{S}$  in rabbit plasma and PC-3 cells.

Cho *et al.* reported a two-photon (TP)  $\text{H}_2\text{S}$  probe **16** for deep tissue imaging.<sup>18</sup> The probe employed 7-(benzo[*d*]thiazol-2'-yl)-9,9-(2-methoxyethoxy)ethyl-9*H*-fluorene as the fluorophore. After reduction by  $\text{H}_2\text{S}$ , the TP absorption cross section of **16** was 302 GM at 750 nm in HEPES buffer. The probe was able to detect endogenous  $\text{H}_2\text{S}$  in HeLa cells and could visualize the overall  $\text{H}_2\text{S}$  distribution at depths of 90–190  $\mu\text{m}$  in a rat hippocampal slice. The products of **16** had  $\Phi = 0.46$ . The detection limit was 5–10  $\mu\text{M}$ . Cho *et al.* next reported another two-photon ratiometric probe **17** for  $\text{H}_2\text{S}$  detection in mitochondria.<sup>19</sup> The detection mechanism of probe **17** was illustrated in Fig. 2b and d. 6-(Benzo[*d*]thiazol-2'-yl)-2-(methylamino)naphthalene was selected as the fluorophore, and 4-azidobenzyl carbamate was chosen as the  $\text{H}_2\text{S}$  response site. The mitochondrial targeting group was a triphenylphosphonium salt. After reduction by  $\text{H}_2\text{S}$ , the fluorophore was released. Under test conditions, probe **17a** showed a shift in emission from 464 nm to 545 nm, and the quantum yields of probe **17a** and its product changed from 0.24 to 0.12. **17b** exhibited a shift in emission from 420 nm to 500 nm, and in quantum yield from 0.23 to 0.50. There was a larger Stokes shift between the probe **17a** and its precursor due to the fact that **17a** had a more stable charge-transfer excited state. The two-photon ratiometric probe can be used to detect mitochondrial  $\text{H}_2\text{S}$  levels in living cells and tissues. The probe **17a** demonstrated the relationship between the cystathionine  $\beta$ -synthase expression level and the  $\text{H}_2\text{S}$  level in astrocytes. Furthermore, the experiments showed that a genetically mutated Parkinson's disease (PD)-related gene could affect  $\text{H}_2\text{S}$  production in the brains of PD patients.

Peng *et al.* and Xu *et al.* reported a two-photon fluorescent probe **18** with near-infrared emission for the detection of  $\text{H}_2\text{S}$ .<sup>20,21</sup> A styrene group was introduced into the fluorophore to extend the conjugation system of the dicyanomethylenedihydrofuran. After reduction by  $\text{H}_2\text{S}$ , the two-photon absorption cross section of **18** was 50 GM at 820 nm in DMSO. The probe could give a 354-fold fluorescence increase upon detection of  $\text{H}_2\text{S}$ . Furthermore, this probe can detect  $\text{H}_2\text{S}$  in commercial fetal bovine serum, MCF-7 cells, HUVEC cells, rat liver cancer slices and ICR mice. The reported detection limit was 3.05  $\mu\text{M}$ .





Zhang *et al.* synthesized a two-photon fluorescent probe **19** for the detection of H<sub>2</sub>S.<sup>22</sup> This probe employed a naphthalene derivative as the two-photon fluorophore. The detection mechanism of probe **19** was shown in Fig. 2b. Probe **19** had a donor- $\pi$ -acceptor (D- $\pi$ -A) structure, and the recognition unit azide acted as the electron withdrawing group which could break the D- $\pi$ -A structure. When H<sub>2</sub>S reduced the azide to an amine, the D- $\pi$ -A structure recovered and the probe emitted strong fluorescence. The TP absorption cross section of product **19** was estimated to be 110.98 GM at 760 nm, and probe **19** showed a 21-fold TP excited fluorescence increase. The probe could be used to detect endogenous H<sub>2</sub>S in HeLa cells, and the detection limit was 20 nM.

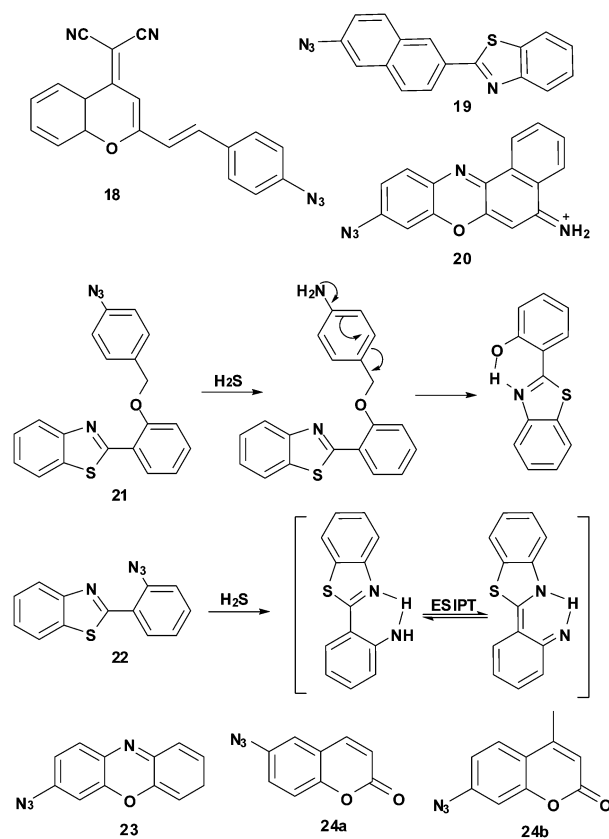
Ma *et al.* reported a cresyl violet-based ratiometric fluorescent probe **20**.<sup>23</sup> The probe also had a donor- $\pi$ -acceptor structure. When the azido group was reduced to an amino group, the D- $\pi$ -A structure changed from electron-withdrawing to electron-donating. The result led to a spectroscopic blue or red shift in emission, which could provide a ratiometric method of H<sub>2</sub>S detection with  $\Phi = 0.44$  and 0.54, respectively. This probe could be used to detect H<sub>2</sub>S in MCF-7 cells and zebrafish by ratiometric imaging. The detection limit of the probe was 0.1  $\mu$ M.

Chang *et al.* reported a ratiometric fluorescent probe **21** based on an excited-state intramolecular proton transfer (ESIPT) mechanism for H<sub>2</sub>S detection.<sup>24</sup> When the azido group was reduced to an amino group, the *p*-aminobenzyl moiety underwent an intramolecular 1,6-elimination to release the ESIPT dye 2-(2'-hydroxyphenyl)-benzothiazole (HBT). The ratio of emission intensity varied 43-fold. The probes based on the ESIPT mechanism often resulted in large Stokes shifts. The ESIPT mechanism could be exploited to design probes based on their unique, environment-sensitive nature. The probe was used to detect H<sub>2</sub>S in HeLa cells, and the detection limit was 2.4  $\mu$ M.

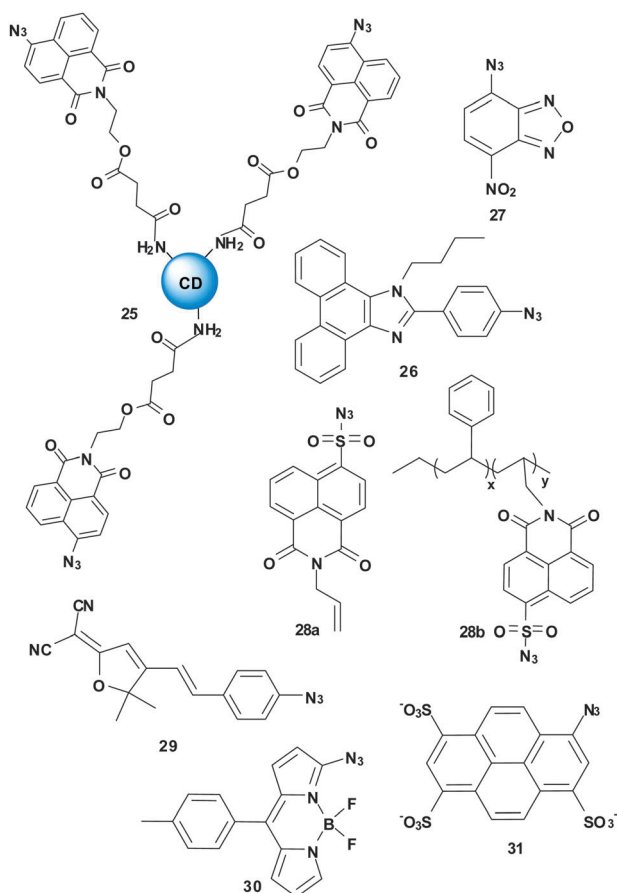
Guo *et al.* reported a fluorescent probe 2-(2-azidophenyl) benzothiazole (**22**) based on the ESIPT mechanism for H<sub>2</sub>S detection.<sup>25</sup> The probe exhibited a 1150-fold increase in fluorescence with

$\Phi = 0.4138$ . The probe was used to detect H<sub>2</sub>S in B16 cells, and the detection limit was 0.78 nM.

Tang *et al.* reported fluorescent probes **23** and **24** for H<sub>2</sub>S detection.<sup>26,27</sup> Probe **23** was synthesized based on the fluorophore phenoxazinone, and showed a 23-fold increase in fluorescence. The probe can detect H<sub>2</sub>S in PBS buffer, fetal bovine serum, and HeLa cells. With coumarin as a fluorophore, these authors reported two-photon fluorescent probes **24a** and **24b** for H<sub>2</sub>S detection. **24b** showed better selectivity and sensitivity than probe **24a**. The product of **24b** gave  $\Phi = 0.88 \pm 0.02$ . Probe **24b** could detect H<sub>2</sub>S from both exogenous addition and possible enzymatic production, and imaging of H<sub>2</sub>S was achieved in the cardiac tissues of normal rats and atherosclerotic rats.



Zeng *et al.* integrated a naphthalimide azide derivative into the anchoring site of carbon nanodots, and developed a fluorescence resonance energy transfer (FRET) ratiometric fluorescent probe **25**.<sup>28</sup> FRET is the interaction between two excited state fluorophores correlated with distance. The process involves the nonradiative transfer of excitation energy from an excited donor to a proximal ground-state acceptor, and it is convenient in the design of ratiometric probes involving the ratio of two emission intensities at different wavelengths. In FRET systems, the emission wavelength of the donor is the excitation wavelength of the acceptor. Therefore, regulation of the precise energy match between carbon nanodots and the naphthalimide azide derivative would be beneficial for H<sub>2</sub>S detection. Probe **25** could detect H<sub>2</sub>S in HeLa and L929 cells, and the detection limit was 10 nM.



Lin *et al.* reported probe **26**, phenanthroimidazole, for H<sub>2</sub>S detection.<sup>29</sup> The azido group could withdraw the electrons from phenanthroimidazole, which made the fluorescence weak. Upon treatment of the probe with H<sub>2</sub>S, the fluorescence of the probe could reach saturation within 3 min. The product of **26** gave  $\Phi = 0.62$ . The probe could be used to detect H<sub>2</sub>S in HeLa cells with a detection limit of  $8.79 \times 10^{-7}$  M.

Chen *et al.* reported 7-nitrobenz-2-oxa-1,3-diazole as a colorimetric and fluorescent probe **27** for H<sub>2</sub>S detection.<sup>30</sup> When the azide was reduced to an amine, probe **27** showed a change in colour from pale-yellow to deep-yellow. The increase of the fluorescence intensity was up to 16-fold. The probe was used to image H<sub>2</sub>S in living MCF-7 cells, and the detection limit was 680 nM.

Wu *et al.* reported the polymer-based fluorescent probe **28** for H<sub>2</sub>S detection.<sup>31</sup> The monomer **28a** could be further functionalized to polymer **28b**. Na<sub>2</sub>S induced a 5-fold and a 3-fold increase in the fluorescence intensity of **28a** and **28b**, respectively. Probe **28b** could detect H<sub>2</sub>S in HeLa cells.

Xu *et al.* reported a fluorescent probe **29** for H<sub>2</sub>S detection based on dicyanomethylenedihydrofuran.<sup>32</sup> **29** gave  $\Phi = 0.018$ , and the probe was able to detect H<sub>2</sub>S in living human umbilical vein endothelial cells.

Talukdar *et al.* designed a colorimetric and fluorometric probe **30** for the detection of H<sub>2</sub>S.<sup>33</sup> The BODIPY-azide could be reduced to a BODIPY-amide by H<sub>2</sub>S with a turn-on fluorescent response. The detection mechanism was as shown in Fig. 2a.

The fluorescence of **30** was quenched by the electron-rich  $\alpha$ -nitrogen of the azido group. The probe displayed a fast response time in serum albumin (within 30 s) with a 28-fold fluorescence increase, and the detection limit was 259 nM. The probe was used to detect H<sub>2</sub>S in HeLa cells.

Hartman *et al.* reported the 8-azidopyrene-1,3,6-trisulfonate probe **31** for H<sub>2</sub>S detection with a 24-fold fluorescence increase.<sup>34</sup> The probe had a high water solubility at concentrations > 100 mM, and could measure H<sub>2</sub>S in serum.

## Fluorescent probes based on reducing nitro groups to amines

There exists a major obstacle in the design of fluorescent probes by exploiting nitro fluorophores, because the nitro group has always been considered to be a strong quencher of fluorophores. However, the nitro group can be reduced by Na<sub>2</sub>S to produce the corresponding amino group under mild conditions, which opens a door to the design and synthesis of new types of fluorescent probe containing a nitro group for H<sub>2</sub>S detection. Taking advantage of this reductive reaction, two main types of H<sub>2</sub>S fluorescent probes have been developed. One type adopts the photoinduced electron transfer (PET) mechanism, which benefits from the strongly electron-withdrawing nature of the nitro group (Fig. 3a). The other type uses the internal charge transfer (ICT) mechanism, which results from a donor- $\pi$ -acceptor structure caused by a strong push-pull electronic effect (Fig. 3b).

Chen *et al.* designed and synthesized a near-infrared fluorescent probe **32** for H<sub>2</sub>S detection in HEPES buffer and in fetal bovine serum.<sup>35</sup> The probe involved the PET mechanism in sensing H<sub>2</sub>S (Fig. 3a). The fluorescence of heptamethine cyanine would be quenched *via* a photoinduced electron transfer (PET) process from the excited fluorophore to the strongly electron-withdrawing nitro group (donor-excited PET; d-PET).<sup>3,36,37</sup> On the other hand, while the nitro group was reduced to an amino group, there might exist an acceptor-excited PET (a-PET) process from the amino group to the excited fluorophore, since the amino group is a strongly electron-donating group with lone-pair electrons.<sup>38,39</sup> However, the probe displayed an increase in fluorescence emission, and the quantum yield increased from 0.05 to 0.11. This phenomenon was attributed to substituent effects; that is, it was not favorable for the substituent in the *meta*-position of the aromatic ring to act as an electron donor. The probe has been used to track H<sub>2</sub>S in RAW264.7 cells.

Li *et al.* reported colorimetric and ratiometric fluorescent probes **33a-c** based on an ICT strategy for the detection of

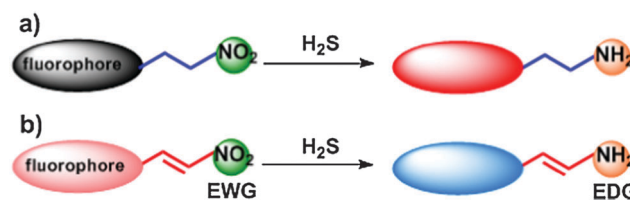
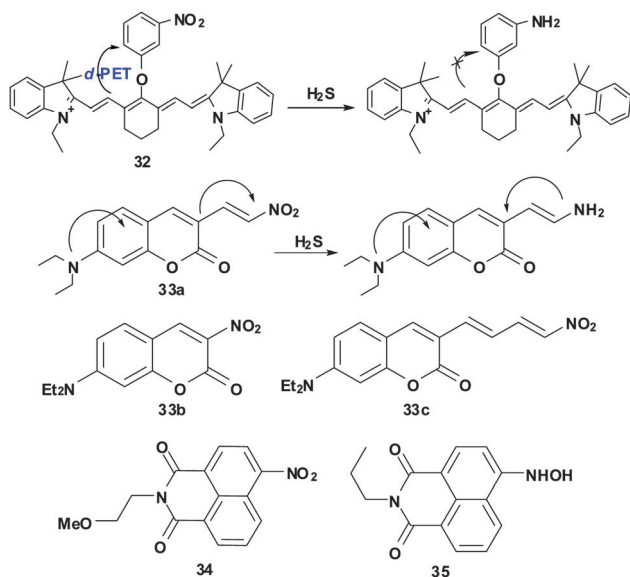


Fig. 3 Summary of strategies for the design of fluorescent probes based on reducing nitro groups to amines.

H<sub>2</sub>S.<sup>40</sup> Probe **33a** demonstrated a typical push-pull electronic system, crossing the coumarin fluorophore. After reaction with H<sub>2</sub>S, the push-pull electron system was blocked by a push-push electron system, which disturbed the ICT mechanism, leading to spectral shifts. The D- $\pi$ -A structures of probes **33a-c** could result in different sensitivities and selectivities. The reaction of probe **33a** with H<sub>2</sub>S resulted in an emission shift from 602 nm ( $\Phi = 0.023$ ) to 482 nm ( $\Phi = 0.236$ ). The detection limit using **33a** was 2.5  $\mu$ M.

Pluth *et al.* reported a 4-nitronaphthalimide fluorescent probe **34** for the detection of H<sub>2</sub>S.<sup>13</sup> The functionalization of the 4-position with amino and nitro in the naphthalimide fluorophore platform resulted in fluorescence turn-on. Probe **34** was also responsive to Cys and GSH. Probe **34** gave  $\Phi = 0.096 \pm 0.001$ , and the probe was used to detect H<sub>2</sub>S in HeLa cells.

Wang *et al.* reported hydroxylamine naphthalimide (**35**) as a fluorescent probe for H<sub>2</sub>S based on the ICT mechanism.<sup>41</sup> During the reduction of nitro groups to amines, hydroxylamine derivatives are produced as intermediates. The hydroxylamine moiety can be reduced more easily than the nitro group. Moreover, the hydroxylamine moiety is an electron-withdrawing group, and can quench the fluorescence of naphthalimide. **35** gave  $\Phi = 0.12$ , and the probe could be used to detect H<sub>2</sub>S in astrocyte cells.



## Fluorescent probes based on reducing selenoxide to selenide

As the active site of the antioxidant enzyme glutathione peroxidase (GPx), organoselenium compounds modulate cellular antioxidant defense systems in defense against damage by reactive oxygen species (ROS) *via* the reduction of reactive oxygen species by biothiols. The oxidation-reduction reaction of the selenoenzyme depends on a unique ping-pong mechanism between selenoxide and selenide.<sup>42</sup> Taking advantage of mimics of the catalytic cycle could aid in the development of fluorescent probes for the reversible detection of H<sub>2</sub>S. Since selenoxide and selenide are electron-withdrawing and electron-donating groups, respectively,

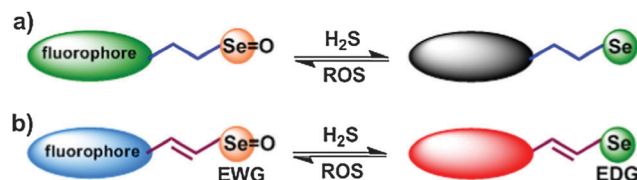


Fig. 4 Summary of strategies for fluorescent probes based on reducing selenoxide to selenide.

fluorescent probes can be smoothly achieved by a photoinduced electron transfer (PET) mechanism (Fig. 4a) and an internal charge transfer (ICT) mechanism (Fig. 4b).

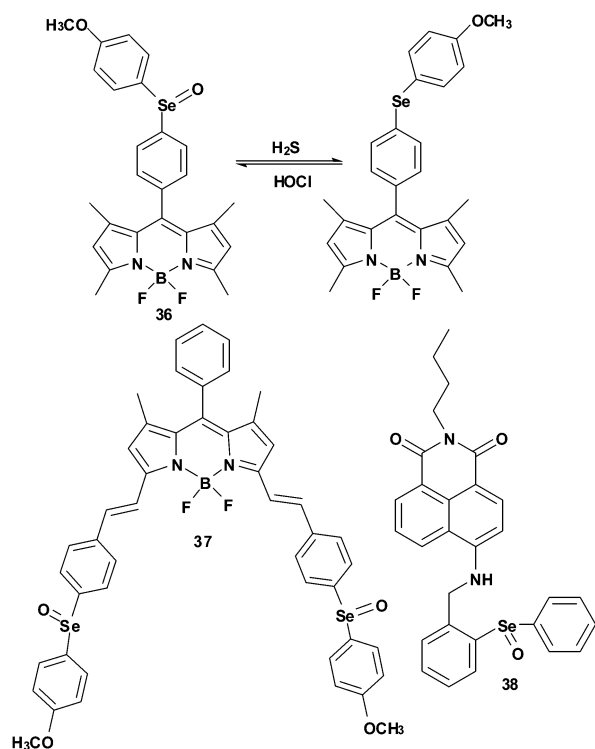
Han *et al.* developed a series of fluorescent probes (**36**, **37**, **38**) containing organoselenium moieties that could be used for monitoring the redox cycles between H<sub>2</sub>S and ROS. The reversible fluorescent probe **36** could detect the redox cycle between HClO and H<sub>2</sub>S. The mechanism was as shown in Fig. 4a. The probe employed a BODIPY fluorophore as the signal transducer and 4-methoxyphenylselenanyl benzene (MPhSe) as the modulator.<sup>43</sup> The fluorescence of **36** was quenched as a result of PET between the modulator and the transducer, but oxidation of Se prevented the PET, causing the fluorescence emission to be “switched on”. The quantum yield increased from 0.13 to 0.96. The probe could be used to detect the redox cycle induced by HClO and H<sub>2</sub>S in RAW264.7 cells.

After integration of the modulator (4-methoxyphenylselenide, MPhSe) into the BODIPY platform through a styrene bridge, probe **37** could function as a near-infrared reversible ratiometric fluorescent probe for the redox cycle between HBrO oxidative stress and H<sub>2</sub>S.<sup>44</sup> The mechanism was as shown in Fig. 4b. This approach could facilitate the D- $\pi$ -A conjugation system and tune the red-shift of the emission efficaciously due to the strong electron-donating properties of the selenide group. After selenide was oxidized to selenoxide by HBrO, the fluorescence of the probe would blue-shift because of the electron-withdrawing effect of selenoxide. The quantum yield increased from 0.00083 to 0.206 (at 635 nm). The probe has been successfully used to detect the HBrO/H<sub>2</sub>S redox cycle in the mouse macrophage cell line RAW264.7.

The probe **38** was based on a 1,8-naphthalimide fluorophore.<sup>45</sup> There exists a PET process in **38** (selenide-form), which was confirmed by time-dependent density functional theory calculations. However, there also was an excited state configuration twist process in the selenide-form, but not in its selenoxide form (**38**). This excited state configuration twist would cause fluorescence quenching. The quantum yield of **38** increased from 0.04 to 0.45. The probe was capable of detecting HOCl oxidative stress and H<sub>2</sub>S reducing repair in RAW 264.7 cells and in mice.

## Fluorescent probes based on the nucleophilic reactions of H<sub>2</sub>S

H<sub>2</sub>S is a reactive nucleophilic species that can participate in nucleophilic substitution *in vivo*. The major challenge in H<sub>2</sub>S detection is to distinguish H<sub>2</sub>S from other biological nucleophiles,



such as cysteine and glutathione, which are present at micromolar or millimolar concentrations inside most cells. The  $pK_a$  of  $H_2S$  is  $\sim 7.0$  in aqueous solution, whereas other bio-thiols have higher  $pK_a$  values (Cys:  $\sim 8.3$ , GSH:  $\sim 9.2$ ). Therefore,  $H_2S$  is considered to be a stronger nucleophile than other biothiols in physiological media.  $H_2S$  can undergo dual nucleophilic reaction as a non-substituted biothiol, however mono-substituted thiols can only undergo one nucleophilic reaction. Based on the nucleophilic and dual nucleophilic properties, fluorescent probes containing bis-electrophilic entities have been devised for  $H_2S$  detection. As shown in Fig. 5a and b,  $H_2S$  can react with the more electrophilic moiety of the fluorescent probe to form an intermediate containing free mercapto ( $-SH$ ). If another electrophilic site is present at a suitable position, such as an *ortho*-ester group or an  $\alpha,\beta$ -unsaturated acrylate group, the  $-SH$  group can undergo Michael addition (Fig. 5a) or a spontaneous cyclization (Fig. 5b) to trigger the fluorescent switch turn-on. The fluorescent probes based on these strategies, as shown in Fig. 5a and b, can also react with other biothiols such as Cys and GSH. However, the intermediates cannot continue to the next cyclization reaction. Therefore, the fluorescent signal does not suffer from the interference caused by other biothiols. As a strong nucleophile,  $H_2S$  also can interrupt the  $\pi$ -conjugation of the probe, thereby leading to a change in the emission wavelength of the probe (Fig. 5c). The removal of the strong electron-withdrawing group by  $H_2S$  can release the fluorophore (Fig. 5d); this strategy is expected to give turn-on fluorescent probes.

#### Fluorescent probes based on Michael addition reaction

Qian *et al.* reported two  $H_2S$ -selective fluorescent probes **39** and **40**.<sup>46</sup> Probe **39** employed BODIPY as the fluorophore, and probe

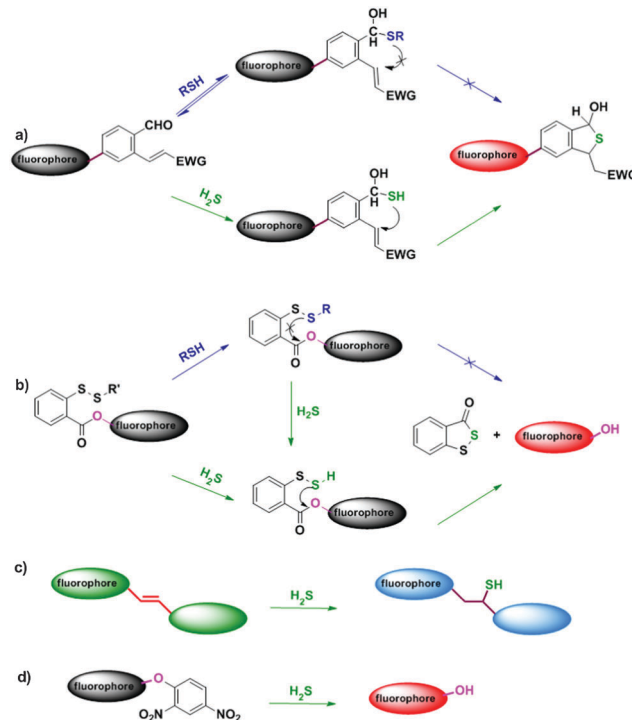


Fig. 5 Summary of strategies for fluorescent probes based on the nucleophilic property of  $H_2S$ .

**40** exploited 1,3,5-triaryl-2-pyrazoline as the fluorophore. The  $H_2S$  recognition moiety consisted of an aromatic framework which was substituted by an  $\alpha,\beta$ -unsaturated acrylate methyl ester and *ortho*-aldehyde ( $-CHO$ ). The aldehyde group could reversibly react with  $H_2S$  to form a hemithioacetal intermediate, which was suitable for Michael addition to the proximal acrylate to yield thioacetal (Fig. 5a). This tandem reaction could block the PET process, and the probe showed a turn-on response to  $H_2S$ . Probes **39** and **40** to  $H_2S$  gave  $\Phi = 0.208$  and  $0.058$ , and these probes could detect  $H_2S$  in HeLa cells.

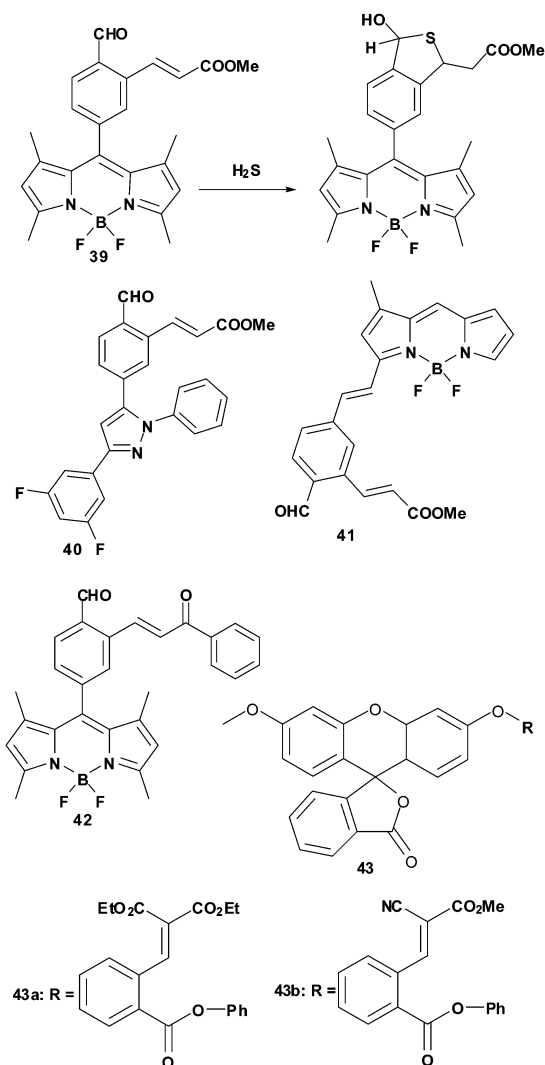
Li *et al.* reported an ICT-based turn-on fluorescent probe **41** for  $H_2S$  detection.<sup>47</sup> The aryl ring substituted by an *ortho*-aldehyde and an  $\alpha,\beta$ -unsaturated acrylate methyl ester was conjugated to the BODIPY fluorophore *via* styrene. The quantum yield increased from 0.006 to 0.13. The probe could detect  $H_2S$  in RAW 264.7 macrophage cells, and the detection limit was  $2.5 \mu M$ .

Zhao *et al.* reported a BODIPY-based probe **42** for  $H_2S$  detection.<sup>48</sup> The probe was designed by replacing the *ortho*-acrylate ester with an  $\alpha,\beta$ -unsaturated phenyl ketone. The probe was able to respond to sulfide in bovine plasma, and the reaction was completed within 120 s at room temperature. **42** gave  $\Phi = 0.10$ . This fast-response probe suggested that the average sulfide concentration in the blood plasma of four mice was  $56.0 \pm 2.5 \mu M$ . The average sulfide concentration in four C57BL/6J mouse brain tissues was estimated to be  $7.1 \pm 1.4 \mu mol g^{-1}$  protein.

Xian *et al.* reported a fluorescent probe **43** for  $H_2S$  detection.<sup>49</sup> The design strategy was based on a Michael addition of



H<sub>2</sub>S followed by an intramolecular cyclization to release the fluorophore. Because biothiols could react readily with Michael acceptors at physiological pH in a rapid equilibrium process, monosubstituted biothiols would not consume the probes in reversible reactions. Probe **43a** and **43b** led to 11-fold and 160-fold turn-on responses, respectively. The probe **43b** could detect H<sub>2</sub>S in COS7 cells, and the detection limit was found to be 1 μM.



### Fluorescent probes based on dual nucleophilic reactions

Xian *et al.* designed a series of turn-on probes (**44**, **45**) to detect H<sub>2</sub>S based on the dual nucleophilic property.<sup>50,51</sup> These fluorescent probes contained reactive disulfide groups. H<sub>2</sub>S could react with the disulfide group to give a free -SH containing intermediate; the intermediate next underwent a spontaneous cyclization to release the fluorophore. Other monosubstituted biothiols, such as Cys and GSH, did not lead to interference. The probe **44** could be used to detect H<sub>2</sub>S in bovine plasma COS7 cells. The fluorescence quantum yield increased from 0.003 to 0.392. Xian *et al.* expanded this strategy to prepare and test the probes **45a–e**. The fluorophores, methoxy fluorescein,

7-hydroxycoumarin, resorufin, and 2-methyl TokyoGreen were chosen as the fluorescent signal transducers. **45d** and **45e** could be used to detect the production of H<sub>2</sub>S from the H<sub>2</sub>S donor YZ-4-074 in HeLa cells. The intensities increased 130-, 275-, 68-, 20-, and 60-fold for **45a–e**, respectively, and the detection limits were determined to be 60, 79, 47, 266, and 47 nm for **45a–e**.

Qian *et al.* reported a ratiometric fluorescent probe **46** based on the excited state intramolecular proton transfer (ESIPT) mechanism for H<sub>2</sub>S detection.<sup>52</sup> The fluorophore 2-(2'-hydroxyphenyl) benzothiazole exhibited ratiometric detection capability, following a large Stokes shift. The recognition reaction completed within 2 min. The probe showed a 30-fold fluorescence increase, and could be used to detect H<sub>2</sub>S in HeLa cells. The detection limit was 0.12 μM.

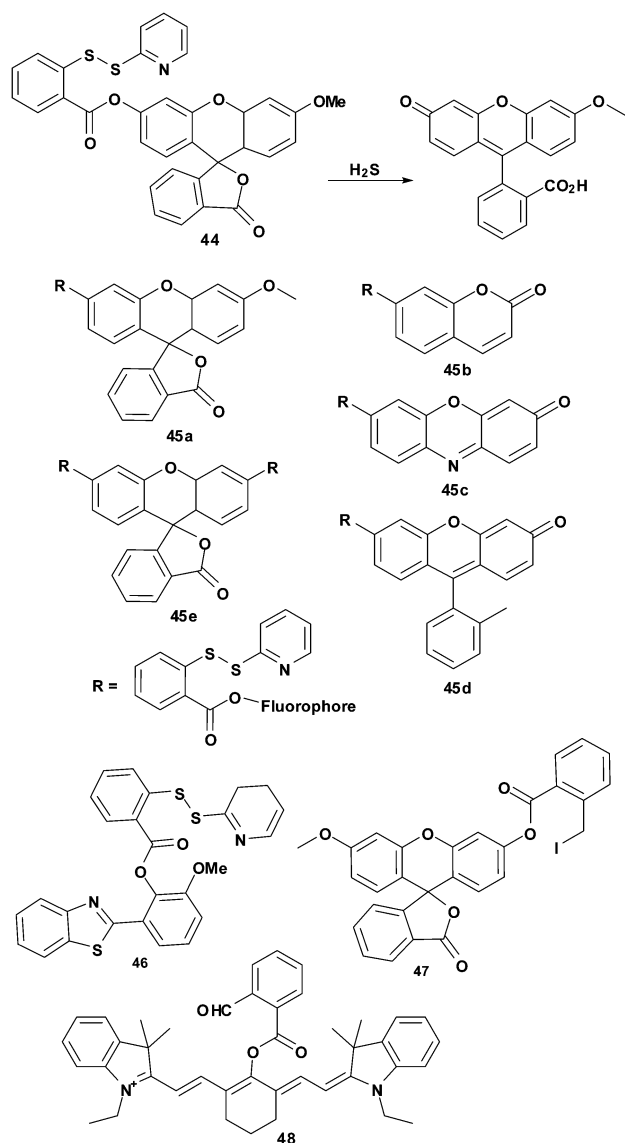
Guo *et al.* reported a methylfluorescein-based probe **47** for the detection of H<sub>2</sub>S.<sup>53</sup> 2-(iodomethyl) benzoate was chosen as the H<sub>2</sub>S trapping group. Upon exposure to H<sub>2</sub>S, the H<sub>2</sub>S-induced substitution–cyclization reaction took place smoothly to release the fluorophore. **47** showed  $\Phi = 0.379$ , and the probe could detect H<sub>2</sub>S in COS-7 cells. The detection limit was 0.10 μM.

Tang *et al.* reported a near-infrared ratiometric fluorescent probe **48** for the detection of H<sub>2</sub>S.<sup>54</sup> 2-Carboxybenzaldehyde was selected as the H<sub>2</sub>S sensing group, with the aldehyde and the ester at the dual nucleophilic addition positions. After reaction with H<sub>2</sub>S, the released fluorophore cyanine benefited from tautomerism between the enol and the ketone forms to allow ratiometric detection. There was a 2500-fold increase in ratio response. The probe could target mitochondria and detect the H<sub>2</sub>S in HepG2 and A549 cells; the detection limit was 5.0–10 nM.

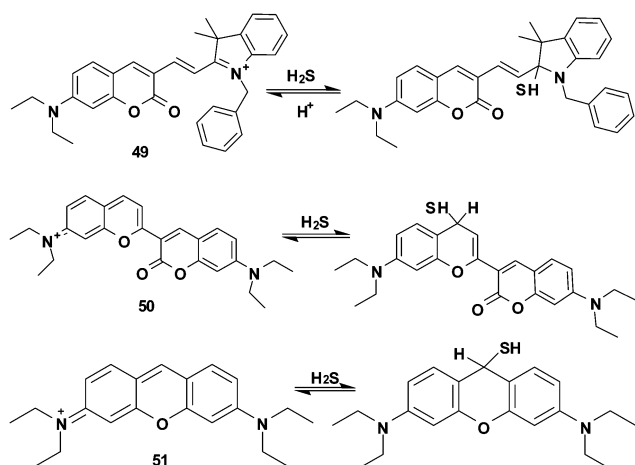
### Fluorescent probes based on a double bond addition reaction

He *et al.* designed a ratiometric fluorescent probe **49** for H<sub>2</sub>S detection.<sup>55</sup> Probe **49** could be considered as a hybrid fluorophore of coumarin and merocyanine through an ethylene group. The probes benefited from the fast HS<sup>-</sup> nucleophilic addition to the merocyanine moiety in a medium of nearly neutral pH. After HS<sup>-</sup>, the main form of H<sub>2</sub>S under physiological conditions, added to the indolenium C-2 atom of **49**, the  $\pi$ -conjugation of the probe was disturbed, eliminating the emission of merocyanine but retaining that of coumarin, causing a shift in the fluorescence spectrum. The probe showed rapid responses to the changes of H<sub>2</sub>S concentration in solution and cells, which were completed within 30 and 80 s, respectively. The intensity ratio of **49** increased over 120-fold. This probe was applied for the detection of changes in the level of H<sub>2</sub>S in the mitochondria of MCF-7 cells.

Guo *et al.* reported a ratiometric fluorescent probe **50** based on a flavylium derivative and a commercially available pyronine dye **51** for H<sub>2</sub>S detection.<sup>56</sup> Probe **50** gave a turn-off response due to the interruption of the  $\pi$ -conjugation of the pyronine ring. The probe could detect H<sub>2</sub>S based on the selective nucleophilic attack of H<sub>2</sub>S on the electrically positive benzopyrylium moiety, which would interrupt the  $\pi$ -conjugation, thereby leading to changes in the emission profile. Probe **50** could provide a ratiometric fluorescent response within 10 s. There



was a 1200-fold increase in the ratiometric value. Probe **50** could be used to detect  $\text{H}_2\text{S}$  in HeLa cells and in human serum; the detection limit was  $0.14 \mu\text{M}$ .



## Fluorescent probes based on a thiolysis reaction

Lin *et al.* synthesized a near-infrared fluorescent probe **52** based on a thiolysis reaction for  $\text{H}_2\text{S}$  detection.<sup>57</sup> The dinitrophenyl group has often been used to protect tyrosine in peptide synthesis. Thiols could remove the dinitrophenyl group under basic conditions. The probe was prepared through condensation of the BODIPY with a Fisher aldehyde, and then caged by 1-fluoro-2,4-dinitrobenzene. The probe is non-fluorescent due to the d-PET process from the excited dye to the strong electron-withdrawing group. After reaction with  $\text{H}_2\text{S}$ , the fluorophore was released with an 18-fold increase in fluorescence. This probe was used to detect  $\text{H}_2\text{S}$  in bovine serum and MCF-7 cells, and the detection limit was  $5 \times 10^{-8} \text{ M}$ .

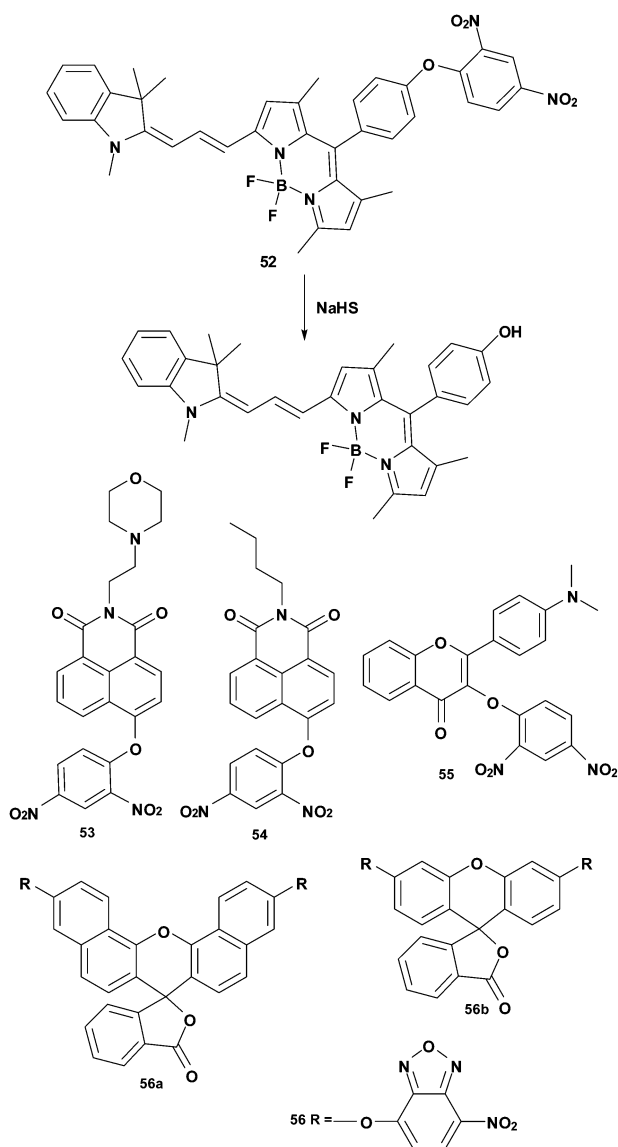
Xu *et al.* reported a lysosome-targeting fluorescent probe **53** for  $\text{H}_2\text{S}$  detection.<sup>58</sup> The probe was prepared by introducing a dinitrophenyl ether group into the 4-position of 1,8-naphthalimide, and 4-(2-aminoethyl)morpholine into the *N*-imide position as the lysosome-targeting group. The lysosome-targeting probe is of significance for the study of the distribution and function of  $\text{H}_2\text{S}$  in lysosomes of living cells. The fluorescence intensity of **53** increased 42-fold. The probe could be used to detect  $\text{H}_2\text{S}$  in the lysosomes of MCF-7 cells. The detection limit was  $0.48 \mu\text{M}$ . Xu *et al.* also developed a 1,8-naphthalimide-derived probe **54** as a two-photon fluorescent probe for  $\text{H}_2\text{S}$  detection based on the thiolysis of dinitrophenyl ether.<sup>59</sup> The fluorescence intensity of **54** increased 37-fold. The probe **54** was applied to detect  $\text{H}_2\text{S}$  in bovine serum and MCF-7 cells, and the detection limit was  $0.18 \mu\text{M}$ .

Feng *et al.* reported a 3-hydroxyflavone-based ESIPT probe **55** for  $\text{H}_2\text{S}$  detection.<sup>60</sup> The emission intensity increased 660-fold when detecting  $\text{H}_2\text{S}$ . The probe could be used to detect  $\text{H}_2\text{S}$  in biological serum and in simulated wastewater samples. The detection limit was  $0.10 \mu\text{M}$ .

Yi *et al.* reported fluorescent probes **56a** and **56b** for  $\text{H}_2\text{S}$  detection, which employed fluorescein and naphthofluorescein as fluorophores.<sup>61</sup> Based on the thiolysis of (7-nitro-1,2,3-benzoxadiazole) ether, the probes could release the fluorophores and give a turn-on response to  $\text{H}_2\text{S}$ . The fluorescence intensity of **56a** and **56b** increased 77-fold and 1000-fold, respectively. The detection limit of **56b** was determined to be  $16 \mu\text{M}$  in solution.

## Fluorescent probes based on copper sulfide precipitation

After forming stable metal complexes with  $\text{Cu(II)}$ , organic chelators have an efficacious quenching effect on fluorophores due to the fact that the paramagnetic  $\text{Cu(II)}$  center can accept the excited state electrons of the fluorophores. It is expected that the removal of  $\text{Cu}^{2+}$  from the complex will result in fluorescence recovery. Such fluorescent probes are often assembled in a fluorophore-chelator-metal ion manner (Fig. 6). According to the hard and soft acids and bases (HSAB) theory,  $\text{S}^{2-}$  has a strong affinity for  $\text{Cu(II)}$ . The  $\text{CuS}$  precipitate is relatively stable, with  $K_{\text{sp}} = 1.26 \times 10^{-36}$ . After the addition of  $\text{H}_2\text{S}$  in solution,



Cu(II) will be eliminated from the complex, and the corresponding fluorescent probes will again become emissive.

Chang *et al.* developed a fluorescent probe 57 for the selective sensing of  $S^{2-}$ .<sup>62</sup> The probe was designed based on a  $Cu^{2+}$  complex of fluorescein containing a dipicolylamine chelator. The detection limit was 420 nM in aqueous solution.

Li *et al.* reported a conjugated polymer fluorescent probe 58 based on a disubstituted polyacetylene containing a dipicolylamine chelator in the side chains for the detection of  $Cu^{2+}$  and  $S^{2-}$ .<sup>63</sup> The fluorescence of the probe could be quenched by  $Cu^{2+}$ . Based on the displacement strategy using  $S^{2-}$  to remove  $Cu^{2+}$ , the quenched fluorescence of the probe could recover. The detection limit was  $5.0 \times 10^{-7} \text{ mol L}^{-1}$ .

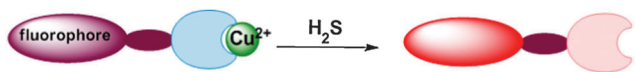


Fig. 6 Summary of the design strategy for fluorescent probes based on copper sulfide precipitation.

Lin *et al.* reported a near-infrared fluorescent probe 59 for  $H_2S$  detection.<sup>64</sup> The probe was composed of a cyanine dye, a piperazine linker and an 8-aminoquinoline ligand. After removal of  $Cu^{2+}$  by  $H_2S$ , the probe gave a turn-on response. The probe 59 showed  $\Phi = 0.11$ , and the detection limit was 280 nM.

Nagano synthesized a series of azamacrocyclic  $Cu^{2+}$ -complex fluorescent probes 60a–d for  $H_2S$  detection.<sup>65</sup> The probe 60b exhibited high sensitivity and selectivity in the detection of  $H_2S$ , and the recognition reaction finished within seconds. It showed a 50-fold fluorescence increase upon the addition of  $H_2S$ . Probe 60b could be used to detect  $H_2S$  produced by 3-mercaptopyruvate sulfurtransferase (3-MST), pseudoenzymatic  $H_2S$  release, and intracellular  $H_2S$  in HeLa cells.

Bai *et al.* reported an 8-hydroxyquinoline-appended fluorescein derivative 61 for  $H_2S$  detection.<sup>66</sup> The fluorescence of the probe was quenched by  $Cu^{2+}$ , which resulted in an off-on type probe for  $S^{2-}$  detection with a 5-fold increase in the fluorescence intensity. The probe was able to reversibly indicate  $S^{2-}$  and  $Cu^{2+}$  changes in turn, and could detect  $H_2S$  in HeLa cells.

Li *et al.* reported a water-soluble fluorescent probe 62 based on a 1,1'-bi-2-naphthol derivative for  $H_2S$  detection.<sup>67</sup> The metal ligand of the probe was 1,4,7,10-tetraazacyclododecane. This probe could recognize  $Cu^{2+}$  and  $S^{2-}$  in an on-off-on mode. The detection limit for the determination of  $S^{2-}$  was  $1.6 \times 10^{-5} \text{ M}$ .

Shen *et al.* designed a fluorescent probe based on phenanthrene-fused dipyrromethene analogue 63 for  $H_2S$  detection.<sup>68</sup> Upon treatment with  $H_2S$ , the probe showed a 14-fold fluorescence increase. The probe could be used as a turn-on fluorescent probe for detecting  $H_2S$  in HeLa cells.

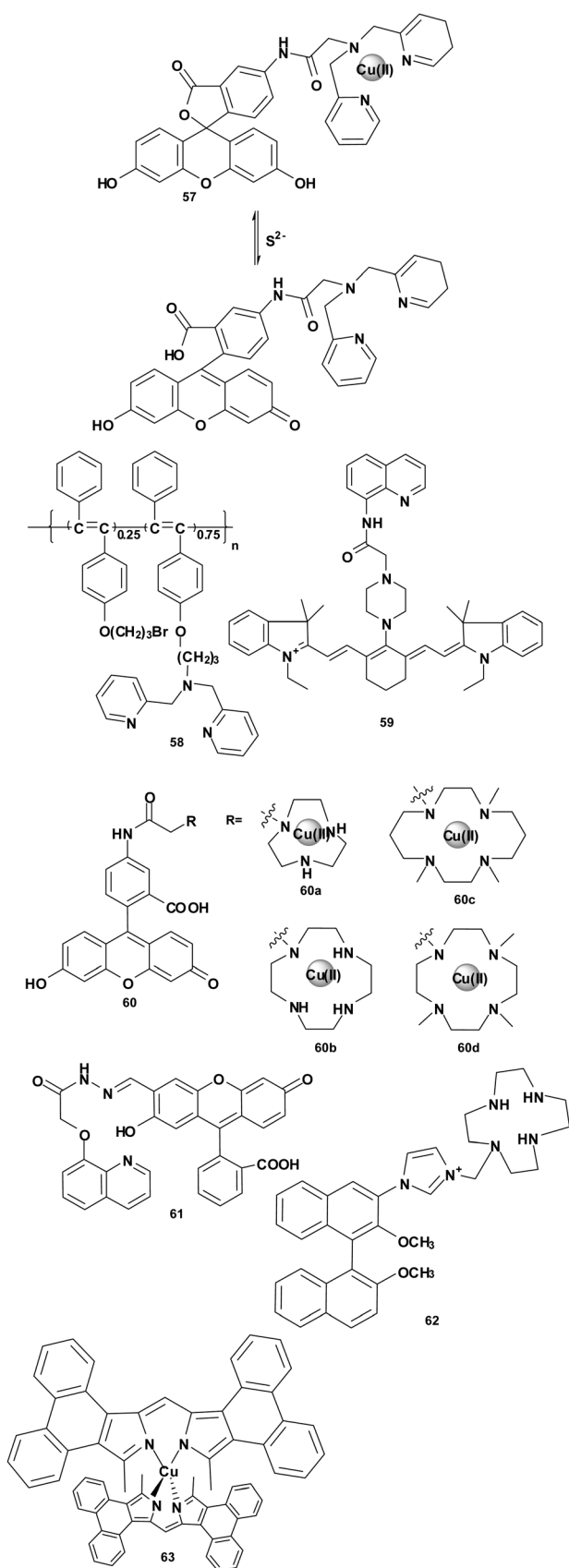
Zang *et al.* designed a water-soluble fluorescent probe for  $H_2S$  detection based on a 3-(1*H*-benzimidazol-2-yl)-2-hydroxybenzoate sodium derivative, 64.<sup>69</sup> The probe was capable of the detection of  $Cu^{2+}$  and  $S^{2-}$  ions at physiological pH. The displacement mechanism the probe employed was supported by the fluorescence lifetime data. Free probe 64 exhibited  $\Phi = 0.1063$ . The detection limitation of  $S^{2-}$  was determined to be  $2.51 \times 10^{-6} \text{ M}$ .

Long *et al.* developed a fluorescent probe 65 for the detection of  $H_2S$  based on the displacement method.<sup>70</sup> The released compound 65 gave a 20-fold fluorescence intensity increase. The probe could be used to detect  $H_2S$  in MCF-7 cells. The detection limit was 0.18  $\mu\text{M}$ .

Zhu *et al.* developed a colorimetric probe 66 based on boron-dipyrromethene- $Cu^{2+}$  for the detection of  $H_2S$  in aqueous media.<sup>71</sup> The probe displayed a 50 nm red-shift in absorption upon the addition of  $H_2S$  in solution. The ratio of the absorbance showed a 34-fold ratiometric increase. The detection limit was  $1.67 \times 10^{-7} \text{ M}$ .

Tang *et al.* reported the 2-(2'-aminophenyl)benzimidazole derivative fluorescent probe 67 for recognition of  $Cu^{2+}$  and  $S^{2-}$  in aqueous solution.<sup>72</sup> The probe displayed an excited-state intramolecular proton transfer (ESIPT) mechanism, and the detection limit was  $9.12 \times 10^{-7} \text{ M}$ .

Ramesh *et al.* synthesized a near-infrared ratiometric indole functionalized rhodamine derivative probe 68 for the detection



of  $\text{Cu}^{2+}$  and  $\text{S}^{2-}$ .<sup>73</sup> The probe employed the resonance energy transfer (RET) mechanism for the detection of  $\text{Cu}^{2+}$ , the process of which involved a donor indole and an acceptor  $\text{Cu}^{2+}$  bound rhodamine moiety. The  $\text{Cu}^{2+}$  complex gave an on-off response in the presence of  $\text{S}^{2-}$ . The Cu-complex probe **68** showed a 600-fold decrease of fluorescence intensity upon the addition of  $\text{S}^{2-}$ . The probe could detect  $\text{Cu}^{2+}$  and  $\text{S}^{2-}$  in HeLa cells.

## Fluorescent probes for sulfane sulfurs

Sulfane sulfurs are the uncharged form of sulfur ( $\text{S}^0$ ), and are attached to proteins through a covalent bond between the  $\text{S}^0$  atom and other sulfur atoms, such as elemental sulfur ( $\text{S}_8$ ), persulfides ( $\text{R-S-SH}$ ), polysulfides ( $\text{R-S}_n\text{-S-R}$ ), thiosulfate ( $\text{S}_2\text{O}_3^{2-}$ ), polythionates ( $\text{S}_n\text{O}_3^{2-}$ ), disulfides and so on.<sup>74-76</sup> As members of the family of reactive sulfur species, sulfane sulfurs exhibit important physiological functions including cellular signal transduction and physiological regulation. The emerging evidence suggests that sulfane sulfurs may be the real signal transduction molecules for cellular events. The rapid production and clearance of  $\text{H}_2\text{S}$  in several biochemical pathways also depends on the metabolic process of sulfane sulfurs.

Xian *et al.* reported fluorescent probes **69**, **70** for the detection of sulfane sulfurs.<sup>77</sup> The detection mechanism was similar to that of probe **44**, which is also illustrated in Fig. 5b. Sulfane sulfur compounds are reactive and labile, and there often exist thiosulfide tautomers. Therefore, a sulfur atom of a sulfane sulfur could react with nucleophilic groups such as the mercapto group to produce a reactive intermediate, which immediately underwent an intermolecular cyclization reaction to release the fluorophore. The fluorescence intensity of both probes increased 50-fold and 25-fold upon the detection of sulfane sulfurs. Probe **69** was used to detect sulfane sulfide both in H9c2 and HeLa cells. The detection limits were 32 nM (for **69**) and 73 nM (for **70**).

## Fluorescent probes for $\text{SO}_2$ and its derivatives

Sulfur dioxide ( $\text{SO}_2$ ) has long been considered as an air pollutant. People who are exposed to  $\text{SO}_2$  may suffer from respiratory diseases and cancer.  $\text{SO}_2$  is rapidly hydrated to sulfite ( $\text{SO}_3^{2-}$ ) and bisulfite ( $\text{HSO}_3^-$ ) in neutral solutions (3 : 1 M/M). However, endogenous  $\text{SO}_2$  can be produced from the degradation of sulfur-containing amino acids.  $\text{SO}_2$ , and its derivatives, may have physiological roles in the regulation of cardiovascular function in synergy with NO. Sulfite is also used in food as an antioxidant to prevent bacterial growth. The design strategies of fluorescent probes for  $\text{SO}_2$  detection are mainly inspired by the nucleophilic properties of  $\text{SO}_2$  (including  $\text{SO}_3^{2-}$  and  $\text{HSO}_3^-$ ). The reaction mechanisms of these fluorescent probes can be sorted according to the nucleophilic addition to aldehydes/ketones (Fig. 7a) and the nucleophilic addition to double bonds (Fig. 7b).  $\text{SO}_2$  and its derivatives selectively add to aldehydes/ketones or to double bonds, leading to changes in the electron-withdrawing effects



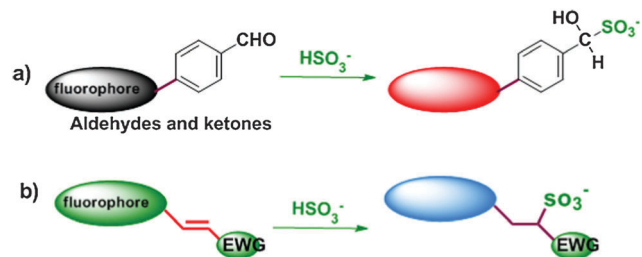
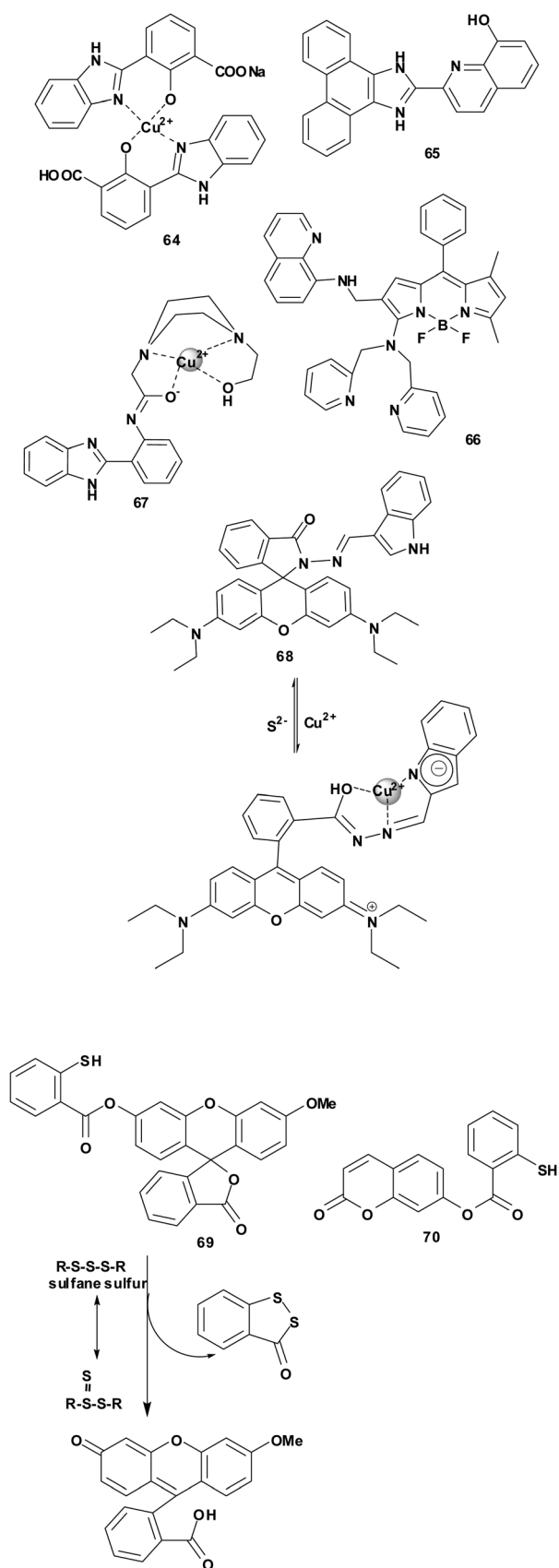


Fig. 7 Summary of strategies for fluorescent probes based on the nucleophilic properties of  $\text{SO}_2$  and its derivatives.

or the  $\pi$ -conjugated systems of the probes, which can cause a response in terms of the fluorescence signal.

### Fluorescent probes based on aldehyde/ketone addition

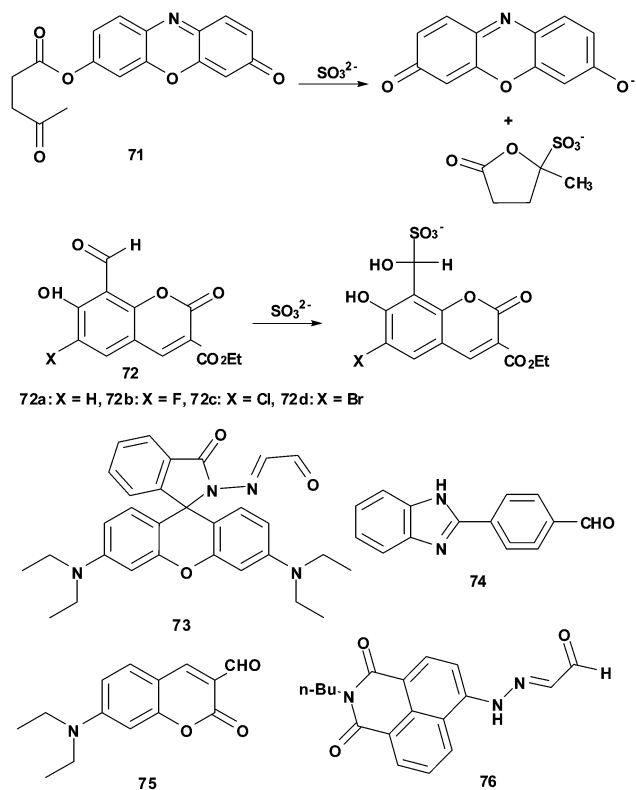
Chang *et al.* reported fluorescent probe 71 for sulfite detection.<sup>78</sup> Sulfite could selectively deprotect the resorufin levulinate moiety of the probe. When sulfite reacted with the carbonyl carbon of the levulinate, a sulfite-added tetrahedral intermediate was formed. The intermediate would next undergo an intermolecular cyclization reaction to release the fluorophore. The fluorescence increase was up to 57-fold. The probe was used to detect sulfite in aqueous solution. The detection limit was  $4.9 \times 10^{-5}$  M.

Guo *et al.* synthesized four coumarin-based fluorescent probes 72a–d for the detection of bisulfite.<sup>79</sup> Bisulfite could selectively attack the aldehyde moieties of the probes. The quantum yields of products of 72a–d were 0.33, 0.62, 0.52 and 0.26, respectively. These probes were used to detect sulfite in granulated sugar. The detection limit was  $1.0 \times 10^{-6}$  M.

Yang *et al.* developed a rhodamine-based fluorescent probe 73 for the detection of bisulfite.<sup>80</sup> Bisulfite could react with the aldehyde to form an aldehyde–bisulfite adduct. Probe 73 also changed from a spirolactam (nonfluorescent) to a ring-opened spirolactam structure, increasing the fluorescence emission. The probe could detect bisulfite in aqueous media. The detection limit was  $8.9 \times 10^{-7}$  M. These authors also presented a ratiometric fluorescent probe 4-(1*H*-benzimidazol-2-yl)benzaldehyde (74) for bisulfite detection.<sup>81</sup> The aldehyde moiety reacted with bisulfite to produce a bisulfite adduct, which resulted in different electron-withdrawing effects and triggered the ICT process. The probe could detect bisulfite in aqueous media. The detection limit was 0.4  $\mu\text{M}$ .

Feng *et al.* developed a coumarin-based fluorescent probe 75 for the detection of bisulfite.<sup>82</sup> The nucleophilic addition reaction with aldehyde would switch-on the fluorescent probe for bisulfite, initiating the ICT process. The aldehyde–bisulfite adduct produced had a quantum yield of 0.43. The probe could detect bisulfite in solution and in HeLa cells. The detection limit was 3.0  $\mu\text{M}$ .

Guo *et al.* designed a C=N isomerization-based fluorescent probe 76 for bisulfite detection.<sup>83</sup> The C=N isomerization could be inhibited by the intramolecular N–H  $\cdots$  N=C hydrogen bond. The formation of the hydrogen bond would block the C=N rotations, and fix the molecular structures in place,



resulting in minimizing the nonradiative energy of the excited state. The quantum yield was 0.374. The probe could detect bisulfite in locally granulated sugar; the detection limit was 0.1  $\mu\text{M}$ .

### Fluorescent probes based on double bond addition

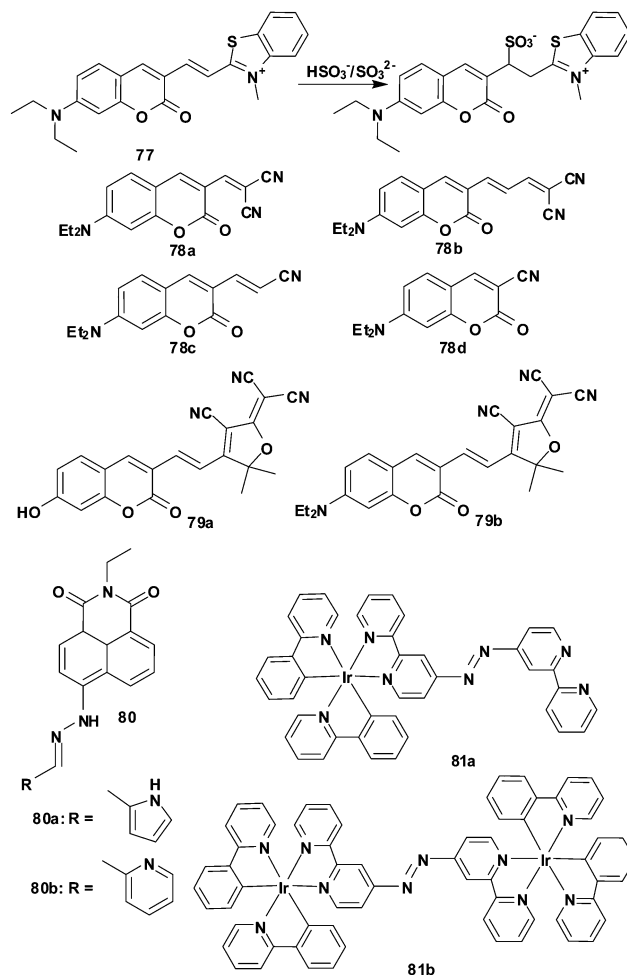
Guo *et al.* reported a coumarin-hemicyanine fluorescent probe 77 for bisulfite and sulfite detection.<sup>84</sup> The nucleophilic attack of  $\text{SO}_3^{2-}/\text{HSO}_3^-$  on the double bond interrupted the  $\pi$ -conjugated structure of probe 77. As a result, the emission profiles before and after adding  $\text{SO}_3^{2-}/\text{HSO}_3^-$  shifted due to the distinct emissions of the coumarin-hemicyanine fluorophore and the produced coumarin fluorophore. The probe gave a 1110-fold increase in the ratiometric signal. The probe could be used to detect  $\text{SO}_3^{2-}/\text{HSO}_3^-$  in HeLa cells. The detection limit was 0.38  $\mu\text{M}$ .

Li *et al.* reported colorimetric and ratiometric fluorescent probes 78a–d for the detection of sulfite.<sup>85</sup> These probes were based on the fluorophore 7-diethylamine coumarin, which conjugated with the cyano group through double bonds. Probes 78a and b provided the best responses to  $\text{SO}_3^{2-}$ .  $\text{SO}_3^{2-}$  underwent a Michael addition to the  $\alpha,\beta$ -unsaturated double bond, which interrupted the intramolecular charge transfer (ICT) process of the probe. The probes could detect sulfite in solution. Probe 78a had a 232-fold intensity ratio increase. The detection limit was 58  $\mu\text{M}$ . The same group also presented near-infrared fluorescent probes 79a and b for the colorimetric and ratiometric detection of  $\text{SO}_2$  derivatives.<sup>86</sup> The probes were composed of coumarin fluorophores and 2-dicyanomethylene-3-cyano-4,5,5-trimethyl-2,5-dihydrofuran, which had three cyano groups. Probe 79a possessed better water solubility and electron-withdrawing properties. The signal ratio at two different

wavelengths could increase 775-fold within 90 seconds. The probe was used to detect  $\text{SO}_2$  derivatives in U-2OS cells, and the detection limit was 0.27 nM.

Weng *et al.* reported fluorescent probes (80a and b) based on 4-hydrazinyl-1,8-naphthalimide for  $\text{SO}_3^{2-}/\text{HSO}_3^-$  detection.<sup>87</sup> The electron donating pyrrole moiety in probe 80a was responsible for fluorescence quenching through the photoinduced electron transfer (PET) process. The  $\text{SO}_3^{2-}/\text{HSO}_3^-$  could form hydrogen bonds with the pyrrole moiety, and the PET process was blocked. Probe 80a gave a 65-fold fluorescent increase upon the detection of sulfite. The probe could be used to monitor the  $\text{SO}_2$  released from an  $\text{SO}_2$  donor in real time and could detect  $\text{SO}_3^{2-}/\text{HSO}_3^-$  in GES-1 cells. The detection limit was 0.56  $\mu\text{M}$ .

Chao *et al.* developed azo group-bridged dinuclear iridium(III) complexes 81a and b as phosphorescent probes for the detection of  $\text{SO}_3^{2-}/\text{HSO}_3^-$ .<sup>88</sup> When the azo group was incorporated into ruthenium(II) complexes, it became more reactive and could react with  $\text{SO}_3^{2-}/\text{HSO}_3^-$ . Moreover, the azo group is an electron-withdrawing group which could quench the luminescence of luminescent metal complexes employing the metal-to-ligand charge-transfer (MLCT) mechanism. After the  $\text{SO}_2$  derivatives underwent nucleophilic addition to the azo group, probe 81b became luminescent. The phosphorescence responses



showed a 26-fold and 27-fold increase for sulfite and bisulfite. Probe **81b** was able to detect external and endogenous  $\text{SO}_3^{2-}/\text{HSO}_3^-$  in HepG2 cells. The detection limits were 0.24  $\mu\text{M}$  for  $\text{SO}_3^{2-}$  and 0.14  $\mu\text{M}$  for  $\text{HSO}_3^-$ .

## Conclusions and prospects

In this feature article, we have summarized the synthetic and design strategies in the development of reaction-based fluorescent probes which are classified by the reaction types between analytes ( $\text{H}_2\text{S}$ , sulfane sulfurs and  $\text{SO}_2$  derivatives) and probes. According to the reaction types, the probes are illustrated through and explained by examples: (a)  $\text{H}_2\text{S}$  reductive reactions: reducing azides to give amines, reducing nitro/azanol to give amines, and reducing selenoxide to give selenide; (b)  $\text{H}_2\text{S}$  nucleophilic reactions: Michael addition reaction, dual nucleophilic reaction, double bond addition reaction, and thiolysis reaction; (c) copper sulfide precipitation reaction. The detection of sulfane sulfurs is mainly based on the nucleophilic addition reaction, and the detection of  $\text{SO}_2$  derivatives is based on the nucleophilic and reductive properties of  $\text{SO}_2$  derivatives.

Rapid recent developments in fluorescent probes for reactive sulfur species will likely prove to further facilitate analysis by fluorescence bioimaging technology. Compared with traditional methods, the detection of reactive sulfur species *via* fluorescence spectrometry can lower the external influence on the endogenous species distribution, can reduce the time of sample preparation, and can achieve real-time detection, in line with the high reactivity of these species. Despite the fact that reaction-based probes deliver us unique and versatile approaches for examining a wide range of reactive species in chemical and biological systems, there also exist many obstacles in terms of new reaction types, selectivity, sensitivity, response time, and fundamental applications. Although the reported detection limits are down to micromolar or even nanomolar levels, fluorescent probes for the detection of original reactive sulfur species and their distribution under normal physiological conditions are very rare. The distribution of reactive sulfur species in cells can be elucidated by probes which have targeting functions, and the quantitative analysis of reactive sulfur species in cells can be resolved by flow cytometry. For example, endogenous  $\text{H}_2\text{S}$  variation is always restricted to a shape range within a short time; we term it as the “ $\text{H}_2\text{S}$  spark” because this is the spontaneous and spatio-temporally localized nature of  $\text{H}_2\text{S}$  biological release. Therefore, to design a probe which can sense the “ $\text{H}_2\text{S}$  spark” will be very meaningful. A similar situation also occurs with other reactive small molecules such as  $\text{NO}$ ,  $\text{H}_2\text{O}_2$ ,  $\text{CO}$ ,  $\text{NH}_3$ ,  $\text{SO}_2$ , and sulfane sulfurs.

Organisms possess a complex environment; the generation and decay of bioreactive species involves various stages. It is desirable to exploit distinctive design schemes that involve reversible chemoselective reactions and catalytic processes which can simulate enzymes. The reversible strategies suffer from many challenges, such as photostability, perturbation of

target molecules, cell leakage, and response frequency. Along these lines, the launch of multiresponse probes for bioimaging detection is also expected, because the reactive small molecules show signaling crosstalk during physiological and pathological processes. Compared with single analyte probes, multiresponse probes will provide facilities for the improvement of diagnostic and therapy tools, and offer important future directions for biological events.

Above all, the development of perfect probes is a challenging task. It requires to master basic concepts and strategies. The development of probes should address key biological problems. Future reaction-based design principles must pay attention to endogenous reactive small molecules under normal physiological conditions. Regardless of the position of the probes in the spectrum (visible region or near-infrared range), desirable probes should respond well to a minor concentration change, give dependable results, and meanwhile avoid interference from native cellular species, particularly biomolecular species such as glutathione and cysteine, and so on. All these will require the probes to exhibit good selectivity, high sensitivity, good photostability, low cytotoxicity, suitable water solubility, and the ability to work within the physiological pH range. Real applications of fluorescent probes, especially in clinical diagnostic imaging, is the ultimate goal.

## Acknowledgements

We thank the NSFC (No. 21275158), the Innovation Projects of CAS (Grant KZCX2-EW-206), and the 100 Talents Program of CAS.

## Notes and references

- 1 M. E. Jun, B. Roy and K. H. Ahn, *Chem. Commun.*, 2011, **47**, 7583–7601.
- 2 J. Chan, S. C. Dodani and C. J. Chang, *Nat. Chem.*, 2012, **4**, 973–984.
- 3 R. Wang, L. Chen, P. Liu, Q. Zhang and Y. Wang, *Chem. – Eur. J.*, 2012, **18**, 11343–11349.
- 4 B. D. Paul and S. H. Snyder, *Nat. Rev. Mol. Cell Biol.*, 2012, **13**, 499–507.
- 5 (a) X. Chen, Y. Zhou, X. Peng and J. Yoon, *Chem. Soc. Rev.*, 2010, **39**, 2120–2135; (b) C. Yin, F. Huo, J. Zhang, R. Martínez-Mañez, Y. Yang, H. Lv and S. Li, *Chem. Soc. Rev.*, 2013, **42**, 6032–6059.
- 6 (a) J. Lu and H. Ma, *Chin. Sci. Bull.*, 2012, **57**, 1462–1471; (b) W. Shi and H. Ma, *Chem. Commun.*, 2012, **48**, 8732–8744; (c) X. Li, X. Gao, W. Shi and H. Ma, *Chem. Rev.*, 2014, **114**, 590–659.
- 7 V. S. Lin and C. J. Chang, *Curr. Opin. Chem. Biol.*, 2012, **16**, 595–601.
- 8 A. R. Lippert, E. J. New and C. J. Chang, *J. Am. Chem. Soc.*, 2011, **133**, 10078–10080.
- 9 V. S. Lin, A. R. Lippert and C. J. Chang, *Proc. Natl. Acad. Sci. U. S. A.*, 2013, **110**, 7131–7135.
- 10 H. Zhang, P. Wang, G. Chen, H.-Y. Cheung and H. Sun, *Tetrahedron Lett.*, 2013, **54**, 4826–4829.
- 11 H. Peng, Y. Cheng, C. Dai, A. L. King, B. L. Predmore, D. J. Lefer and B. Wang, *Angew. Chem., Int. Ed.*, 2011, **50**, 9672–9675.
- 12 T. S. Bailey and M. D. Pluth, *J. Am. Chem. Soc.*, 2013, **135**, 16697–16704.
- 13 L. A. Montoya and M. D. Pluth, *Chem. Commun.*, 2012, **48**, 4767–4769.
- 14 S. Chen, Z. Chen, W. Ren and H. Ai, *J. Am. Chem. Soc.*, 2012, **134**, 9589–9592.
- 15 Z. Wu, Z. Li, L. Yang, J. Han and S. Han, *Chem. Commun.*, 2012, **48**, 10120–10122.

- 16 F. Yu, P. Li, P. Song, B. Wang, J. Zhao and K. Han, *Chem. Commun.*, 2012, **48**, 2852–2854.
- 17 W. Li, W. Sun, X. Yu, L. Du and M. Li, *J. Fluoresc.*, 2013, **23**, 181–186.
- 18 S. K. Das, C. S. Lim, S. Y. Yang, J. H. Han and B. R. Cho, *Chem. Commun.*, 2012, **48**, 8395–8397.
- 19 S. K. Bae, C. H. Heo, D. J. Choi, D. Sen, E. H. Joe, B. R. Cho and H. M. Kim, *J. Am. Chem. Soc.*, 2013, **135**, 9915–9923.
- 20 W. Sun, J. Fan, C. Hu, J. Cao, H. Zhang, X. Xiong, J. Wang, S. Cui, S. Sun and X. Peng, *Chem. Commun.*, 2013, **49**, 3890–3892.
- 21 Y. Zheng, M. Zhao, Q. Qiao, H. Liu, H. Lang and Z. Xu, *Dyes Pigm.*, 2013, **98**, 367–371.
- 22 G. J. Mao, T. T. Wei, X. X. Wang, S. Y. Huan, D. Q. Lu, J. Zhang, X. B. Zhang, W. Tan, G. L. Shen and R. Q. Yu, *Anal. Chem.*, 2013, **85**, 7875–7881.
- 23 Q. Wan, Y. Song, Z. Li, X. Gao and H. Ma, *Chem. Commun.*, 2013, **49**, 502–504.
- 24 Y. Jjiang, Q. Wu and X. Chang, *Talanta*, 2014, **121**, 122–126.
- 25 J. Zhang and W. Guo, *Chem. Commun.*, 2014, **50**, 4214–4217.
- 26 B. Chen, C. Lv and X. Tang, *Anal. Bioanal. Chem.*, 2012, **404**, 1919–1923.
- 27 B. Chen, W. Li, C. Lv, M. Zhao, H. Jin, H. Jin, J. Du, L. Zhang and X. Tang, *Analyst*, 2013, **138**, 946–951.
- 28 C. Yu, X. Li, F. Zeng, F. Zheng and S. Wu, *Chem. Commun.*, 2013, **49**, 403–405.
- 29 K. Zheng, W. Lin and L. Tan, *Org. Biomol. Chem.*, 2012, **10**, 9683–9688.
- 30 G. Zhou, H. Wang, Y. Ma and X. Chen, *Tetrahedron*, 2013, **69**, 867–870.
- 31 K. Sun, X. Liu, Y. Wang and Z. Wu, *RSC Adv.*, 2013, **3**, 14543–14548.
- 32 T. Chen, Y. Zheng, Z. Xu, M. Zhao, Y. Xu and J. Cui, *Tetrahedron Lett.*, 2013, **54**, 2980–2982.
- 33 T. Saha, D. Kand and P. Talukdar, *Org. Biomol. Chem.*, 2013, **11**, 8166–8170.
- 34 M. C. Hartman and M. M. Dcona, *Analyst*, 2012, **137**, 4910–4912.
- 35 R. Wang, F. Yu, L. Chen, H. Chen, L. Wang and W. Zhang, *Chem. Commun.*, 2012, **48**, 11757–11759.
- 36 F. Yu, P. Song, P. Li, B. Wang and K. Han, *Chem. Commun.*, 2012, **48**, 7735–7737.
- 37 F. Yu, P. Li, P. Song, B. Wang, J. Zhao and K. Han, *Chem. Commun.*, 2012, **48**, 4980–4982.
- 38 F. Yu, P. Li, B. Wang and K. Han, *J. Am. Chem. Soc.*, 2013, **135**, 7674–7680.
- 39 E. Sasaki, H. Kojima, H. Nishimatsu, Y. Urano, K. Kikuchi, Y. Hirata and T. Nagano, *J. Am. Chem. Soc.*, 2005, **127**, 3684–3685.
- 40 M. Wu, K. Li, J. Hou, Z. Huang and X. Yu, *Org. Biomol. Chem.*, 2012, **10**, 8342–8347.
- 41 W. Xuan, R. Pan, Y. Cao, K. Liu and W. Wang, *Chem. Commun.*, 2012, **48**, 10669–10671.
- 42 F. Yu, P. Li, G. Li, G. Zhao, T. Chu and K. Han, *J. Am. Chem. Soc.*, 2011, **133**, 11030–11033.
- 43 B. Wang, P. Li, F. Yu, P. Song, X. Sun, S. Yang, Z. Lou and K. Han, *Chem. Commun.*, 2013, **49**, 1014–1016.
- 44 B. Wang, P. Li, F. Yu, J. Chen, Z. Qu and K. Han, *Chem. Commun.*, 2013, **49**, 5790–5792.
- 45 Z. Lou, P. Li, Q. Pan and K. Han, *Chem. Commun.*, 2013, **49**, 2445–2447.
- 46 Y. Qian, J. Karpus, O. Kabil, S. Y. Zhang, H. L. Zhu, R. Banerjee, J. Zhao and C. He, *Nat. Commun.*, 2011, **2**, 495–501.
- 47 X. Li, S. Zhang, J. Cao, N. Xie, T. Liu, B. Yang, Q. He and Y. Hu, *Chem. Commun.*, 2013, **49**, 8656–8658.
- 48 Y. Qian, L. Zhang, S. Ding, X. Deng, C. He, X. E. Zheng, H.-L. Zhu and J. Zhao, *Chem. Sci.*, 2012, **3**, 2920.
- 49 C. Liu, B. Peng, S. Li, C.-M. Park, A. R. Whorton and M. Xian, *Org. Lett.*, 2012, **14**, 2184–2187.
- 50 C. Liu, J. Pan, S. Li, Y. Zhao, L. Y. Wu, C. E. Berkman, A. R. Whorton and M. Xian, *Angew. Chem., Int. Ed.*, 2011, **123**, 10511–10513.
- 51 B. Peng, W. Chen, C. Liu, E. W. Rosser, A. Pacheco, Y. Zhao, H. C. Aguilar and M. Xian, *Chem. – Eur. J.*, 2014, **20**, 1010–1016.
- 52 Z. Xu, L. Xu, J. Zhou, Y. Xu, W. Zhu and X. Qian, *Chem. Commun.*, 2012, **48**, 10871–10873.
- 53 J. Zhang, Y.-Q. Sun, J. Liu, Y. Shi and W. Guo, *Chem. Commun.*, 2013, **49**, 11305–11307.
- 54 X. Wang, J. Sun, W. Zhang, X. Ma, J. Lv and B. Tang, *Chem. Sci.*, 2013, **4**, 2551–2556.
- 55 Y. Chen, C. Zhu, Z. Yang, J. Chen, Y. He, Y. Jiao, W. He, L. Qiu, J. Cen and Z. Guo, *Angew. Chem., Int. Ed.*, 2013, **125**, 1732–1735.
- 56 J. Liu, Y. Q. Sun, J. Zhang, T. Yang, J. Cao, L. Zhang and W. Guo, *Chem. – Eur. J.*, 2013, **19**, 4717–4722.
- 57 X. Cao, W. Lin, K. Zheng and L. He, *Chem. Commun.*, 2012, **48**, 10529–10531.
- 58 Z. Xu, T. Liu, D. R. Spring and J. Cui, *Org. Lett.*, 2013, **15**, 2310–2313.
- 59 T. Liu, X. Zhang, Q. Qiao, C. Zou, L. Feng, J. Cui and Z. Xu, *Dyes Pigm.*, 2013, **99**, 537–542.
- 60 Y. Liu and G. Feng, *Org. Biomol. Chem.*, 2014, **12**, 438–445.
- 61 C. Wei, Q. Zhu, W. Liu, W. Chen, Z. Xi and L. Yi, *Org. Biomol. Chem.*, 2014, **12**, 479–485.
- 62 M. G. Choi, S. Cha, H. Lee, H. L. Jeon and S. K. Chang, *Chem. Commun.*, 2009, 7390–7392.
- 63 L. Zhang, X. Lou, Y. Yu, J. Qin and Z. Li, *Macromolecules*, 2011, **44**, 5186–5193.
- 64 X. Cao, W. Lin and L. He, *Org. Lett.*, 2011, **13**, 4716–4719.
- 65 K. Sasaki, K. Hanaoka, N. Shibuya, Y. Mikami, Y. Kimura, T. Komatsu, T. Ueno, T. Terai, H. Kimura and T. Nagano, *J. Am. Chem. Soc.*, 2011, **133**, 18003–18005.
- 66 F. Hou, L. Huang, P. Xi, J. Cheng, X. Zhao, G. Xie, Y. Shi, F. Cheng, X. Yao, D. Bai and Z. Zeng, *Inorg. Chem.*, 2012, **51**, 2454–2460.
- 67 M. Q. Wang, K. Li, J. T. Hou, M. Y. Wu, Z. Huang and X. Q. Yu, *J. Org. Chem.*, 2012, **77**, 8350–8354.
- 68 X. Qu, C. Li, H. Chen, J. Mack, Z. Guo and Z. Shen, *Chem. Commun.*, 2013, **49**, 7510–7512.
- 69 Y. Fu, Q.-C. Feng, X.-J. Jiang, H. Xu, M. Li and S.-Q. Zang, *Dalton Trans.*, 2014, **43**, 5815–5822.
- 70 J. Wang, L. Long, D. Xie and Y. Zhan, *J. Lumin.*, 2013, **139**, 40–46.
- 71 X. Gu, C. Liu, Y.-C. Zhu and Y.-Z. Zhu, *Tetrahedron Lett.*, 2011, **52**, 5000–5003.
- 72 L. Tang, X. Dai, M. Cai, J. Zhao, P. Zhou and Z. Huang, *Spectrochim. Acta, Part A*, 2014, **122**, 656–660.
- 73 C. Kar, M. D. Adhikari, A. Ramesh and G. Das, *Inorg. Chem.*, 2013, **52**, 743–752.
- 74 B. D. Paul and S. H. Snyder, *Nat. Rev. Mol. Cell Biol.*, 2012, **13**, 499–507.
- 75 J. I. Toohey, *Anal. Biochem.*, 2011, **413**, 1–7.
- 76 R. Greiner, Z. Palinkas, K. Basell, D. Becher, H. Antelmann, P. Nagy and T. P. Dick, *Antioxid. Redox Signaling*, 2013, **19**, 1749–1765.
- 77 W. Chen, C. Liu, B. Peng, Y. Zhao, A. Pacheco and M. Xian, *Chem. Sci.*, 2013, **4**, 2892–2896.
- 78 M. G. Choi, J. Hwang, S. Eor and S.-K. Chang, *Org. Lett.*, 2010, **12**, 5624–5627.
- 79 K. Chen, Y. Guo, Z. Lu, B. Yang and Z. Shi, *Chin. J. Chem.*, 2010, **28**, 55–60.
- 80 X. Yang, M. Zhao and G. Wang, *Sens. Actuators, B*, 2011, **152**, 8–13.
- 81 G. Wang, H. Qi and X. F. Yang, *Luminescence*, 2013, **28**, 97–101.
- 82 X. Cheng, H. Jia, J. Feng, J. Qin and Z. Li, *J. Mater. Chem. B*, 2013, **1**, 4110–4114.
- 83 Y. Sun, P. Wang, J. Liu, J. Zhang and W. Guo, *Analyst*, 2012, **137**, 3430–3433.
- 84 Y. Sun, J. Liu, J. Zhang, T. Yang and W. Guo, *Chem. Commun.*, 2013, **49**, 2637–2639.
- 85 M. Wu, T. He, K. Li, M.-B. Wu, Z. Huang and X.-Q. Yu, *Analyst*, 2013, **138**, 3018–3025.
- 86 M. Wu, K. Li, C.-Y. Li, J.-T. Hou and X.-Q. Yu, *Chem. Commun.*, 2014, **50**, 183–185.
- 87 C. Wang, S. Feng, L. Wu, S. Yan, C. Zhong, P. Guo, R. Huang, X. Wang and X. Zhou, *Sens. Actuators, B*, 2014, **190**, 792–799.
- 88 G. Li, Y. Chen, J. Wang, Q. Lin, J. Zhao, L. Ji and H. Chao, *Chem. Sci.*, 2013, **4**, 4426–4433.